Stephen F. Austin State University

SFA ScholarWorks

Spring 5-8-2021

Radiosonde High Altitude Measurements of Radiation Levels and Cosmic Ray Events

AYODEJI OPEYEMI AKINULIOLA
Stephen F. Austin State University, ayodejiheph@gmail.com

Follow this and additional works at: https://scholarworks.sfasu.edu/etds

Part of the Atmospheric Sciences Commons, and the Engineering Physics Commons

Tell us how this article helped you.

Radiosonde High Altitude Measurements of Radiation Levels and Cosmic Ray Events

Creative Commons License

RADIOSONDE HIGH ALTITUDE MEASUREMENTS OF RADIATION LEVELS

AND COSMIC RAY EVENTS

By

Ayodeji O. Akinuliola

Presented to the Faculty of the Graduate School of

Stephen F. Austin State University

In Partial Fulfillment

Of the Requirements

For the Degree of

Master of Science

STEPHEN F. AUSTIN STATE UNIVERSITY

May 2021

RADIOSONDE HIGH ALTITUDE MEASUREMENTS OF RADIATION LEVELS

AND COSMIC RAY EVENTS

By

Ayodeji O. Akinuliola, B.S.

APPROVED:

_____
Dr. W. D. Bruton, Thesis Director

_____
Dr. James T. Adams, Committee Member

_____
Dr. Robert Friedfeld, Committee Member

_____
Dr. Matthew A. Beauregard, Committee Member

_____
Dr. Pauline Sampson
Dean of Research and Graduate Studies

ABSTRACT

Just above us, cosmic rays are hurtling in from space. These fast-moving particles crash uncontrollably into molecules in the atmosphere, causing spontaneous decays of these particles. Despite the fact that we are broadly shielded from this radiation on earth, these particles can still disturb humans and electronics alike. Therefore, this research focuses on expanding the use of long-range radio transmitters such as radiosondes to transmit valuable data such as cosmic ray flux, geographical position, atmospheric temperature, pressure, etc. This can improve real-time radiation monitoring for aviation industry crew and passengers working in potentially higher radiation environments. On March 11, 2021 the balloon's volume was gradually enlarged, and was released at 11:52:13 AM and the balloon travelled a total range of 285 km which is the longest range travelled by any balloon launched at SFA. It attained an altitude of about 30,000 km.

ACKNOWLEDGMENTS

I am extremely thankful for the completion of my thesis and for the experiences through graduate school at Stephen F. Austin State University, which is 6443 miles away from my home country Nigeria. Coming to America to study was one of my big dreams, I am delighted that I came, I saw and conquered. All dreams and aspirations will come to reality if we learn to lean on the support of the creator of the all universal. Firstly, I am thankful to God for being on my side all the way.

I am deeply indebted to my parents Benson and Taiwo Akinuliola, for their enormous support from birth till this age. I must say, It is a blessing to have you as my parents.

My siblings Akinbobola, Abimbola, and Ayoola, you guys have been great too. Thank you for being there to make me smile and laugh when the journey was tough.

My success story wouldn't be complete if I fail in mentioning the family of Olusoji and Olajiire Fatokun, you made me feel at home here in the United States. You showed me great love and acceptance. You are the best!

Every successful person has at least one friend that believes in their dream and helps in every way possible to achieve it. Oluwaseun Farotimi (PhD in

Mathematics), took it upon himself to help me from the first day I said I was to pursue a Master degree in Physics even till now. May God reward your labor of love.

Dr. Dan Bruton, my thesis advisor, from the very first day I met him, you are a selfless professor who enjoys helping students achieve their academic goals. I would say he is a father figure to me in the department.

To all my professors who taught me through my academic stay at SFA, I am grateful and I am appreciative.

To my African community here in Nacogdoches, Oluwadamilola Fateru, Chika, Efosa, Niyi, Ayo, Oluwaseun, Udeme, and Mimi, Thank you for making my stay here at SFA worth it.

In conclusion, I greatly appreciate you all for being there to nurture my academic career. You are the best gift given to me by God.

TABLE OF CONTENTS

LIST OF FIGURES

LIST OF TABLES

CHAPTER ONE

<u>INTRODUCTION</u>

Earth's atmospheric region that lies between 20 km and 100 km (65,000 and 328,000 feet) above sea level is called *Near Space* and is encompassed by the stratosphere, mesosphere, and lower thermosphere. At 50,000 feet and above, the pressure becomes very low, and humans cannot survive without a pressurized suit. Despite this limitation, humans have an unending appetite for exploring the unknown, discovering new worlds, pushing the boundaries of our scientific knowledge and technical limits, and then pushing further. One of the solutions humans have devised to access these great heights is a high-altitude balloon carrying environmental sensors.

High-altitude balloons are usually filled with helium or hydrogen, or in some cases methane, before they are launched into the stratosphere. The history of modern balloons dates back to 1766 when Joseph Black proposed that a balloon filled with hydrogen would be able to rise in the air. The balloon was named Charlière and was filled with hydrogen, which had only been produced in small quantities. The hydrogen was made by the mixture of 540 kg (1,190 lb) of iron and 270 kg (600 lb) of sulfuric acid. It took five days for Charlière to get filled, and 300,000 spectators viewed this public experiment

at Champ de Mars in Paris. Charlière was launched, and it rose through the clouds and descended 45 minutes later, about 20 km (12 mi) away from Paris.

High-altitude balloons could be manned or unmanned. The manned balloons have been in use from the 1930's to 1960's for research and to seek flight altitude records. Some remarkable human-crewed high altitude balloon flights include Project Excelsior by Joseph Kittinger in 1960 at an altitude of 31,300 meters, the Red Bull Stratos by Felix Baumgartner in 2012 at an altitude of 38,969 meters, and the most recent by Alan Eustace in 2014 an altitude of 41,419 meters.

Unmanned high-altitude balloons (HABs) are massively used as research balloons. They are regularly utilized as weather balloons, as well as for atmospheric and climate research. They are also regularly used to collect data and imagery from near space. For this research, the focus will be on unmanned high-altitude balloons.

Just above us, cosmic rays are hurtling in from outer space. These fast moving particles crash uncontrollably into molecules in the atmosphere, causing a spontaneous decays of these particles. Despite the fact that we are broadly shielded from this radiation on earth, these particles can still disturb humans and electronics alike. Therefore, this research focuses on using radiosondes to measure the radiation in the atmosphere as the balloon travels to near space as this will improve real-time radiation monitoring for aviation

industry crew and passengers working in potentially higher radiation environments.

One of the foreseen challenges in the recovery of the payloads is that the payloads may land in remote areas or areas that humans cannot access because of the terrain. Therefore, it will be advantageous to transmit the data rather than travel to those inaccessible terrains to recover the payload's memory card. Therefore, the two main goals are: (1) to expand the data payload to include cosmic radiation measurements and (2) to transmit the telemetry and sensor data during flight.

OBJECTIVES

1. Use a long-range radio transmitter to obtain valuable data about the HAB while in flight and landing.
2. Obtain the location (latitude and longitude), altitude, temperature, images, pressure, speed, and other information about the balloon.
3. Obtain and analyze the cosmic ray readings at high altitude as the balloon floats in the atmosphere using the radiosonde.
4. Use a radiosonde to measure and calculate the wind speed, pressure, relative humidity, altitude, pressure, temperature, relative humidity, wind direction, and geographical position "latitude or longitude".

5. Demonstrate that an instrument that costs less than $1000 can help collect Geiger counter readings up at altitude up to to 20 miles.

6. Predict the path of the high-altitude balloon.

7. Measure the temperature, pressure, radiation (versus altitude).

8. Build payloads that can be recycled with low cost and low risk, which is difficult to achieve by satellites.

9. Test and analyze the results obtained from the device and make future predictions about the nature of radiation in the Earth's atmosphere.

LITERATURE REVIEW

Since the late 18th century, high-altitude balloons (HABs) have provided an essential platform for scientific investigations and observations. Scientists have since then used these balloons to collect data from unprecedented altitudes. These balloon-based experiments helped in the early studies of cosmic ray circulation all over the atmosphere and allowed the first direct measurements of the stratosphere (Yajima et al., 2004). The expansion of HABs' utility, has become indispensable to astrophysical, planetary, and climate studies, including radiation investigations in Near Space environments (Lawrence et al., 2018), surveillance of atmospheric ozone levels (Hofmann et al., 1987), and measurement of electric fields within the stratosphere (Gurubaran et al., 2017).

In 1783, the Montgolfier brothers heralded a new age of transportation and exploration when they used hot air to drive an untethered balloon to an altitude of approximately 2 km. The balloon was made from sackcloth and held together with cords. This balloon challenged the way we thought about human travel, and it has since evolved into a booming platform for carrying out novel science and testing new technologies. Today, remarkable progress has been made in the development of high-altitude balloons, such as the ability to reach a height of 40 km and it can now support more than 3000 kg in mass of payload. Long-duration balloons can now support missions lasting up to 55 days in duration.   Development of balloon technologies (i.e., Super-Pressure Balloons) are expected to increase the span to 100 days or longer; competing with satellite payloads. National Aeronautics and Space Administration (NASA) is an independent agency that supports a broad range of science payloads, spanning multiple disciplines (astrophysics, heliophysics, planetary, and earth science.) Applications extending beyond traditional science include testing new technologies for future space-based application and stratospheric airships for planetary applications. NASA continues to provide a training ground for the next generation of scientists and engineers.

A group of researchers conducted an extensive experiment titled "An Overview of High-Altitude Balloon Experiments" (Margarita et al., 2014)., at the Indian Institute of Astrophysics they worked with a total of nine free-flying

balloons from March 2013 to November 2014. They encountered many challenges such as loss of signal using GSM-GPS tracker, failure of the attitude sensor, the battery drainage due to low temperature, and the failure of the time-based Flight Termination Unit (FTU), due to a nichrome wire break. They had to use three different balloons at the ninth launch because the first balloon burst prematurely within 20 mins of the launch, while the other two balloons burst 90 mins after the launch. At the end of the experiment, the maximum altitude achieved was estimated to be 26 km. They successfully obtained the data, including temperature readings and the scattered solar spectrum at different times during this flight. They intended to use collected flight data to model the performance of the flight with multiple balloons, analyze the scattered solar UV spectra, detect the airglow lines and establish the altitude dependence of the strength of the lines, to reduce the payload's weight and establish the dependence of the ascent or descent rates on the number of balloons, gas volume, and payload weight. The key research questions for this type of research are:

1. Can high-altitude radiation measurements be made with low equipment costs so that the experiment can be repeated multiple times?

2. Are there significant changes in the radiation levels detected for various altitudes over time?

CHAPTER TWO

THEORY AND INSTRUMENTATION

<u>Alpha Particles</u>

The alpha particles ($\boldsymbol{\alpha}$) comprise two neutrons and two protons bound together into a particle identical to a helium-4 nucleus. Alpha particles are named after the first letter in the Greek alphabet, α, and α++ denotes it. Alpha particles were the first nuclear radiation to be discovered and were named by Ernest Rutherford in 1899. He and his coworkers used alpha particles in experiments to probe the structure of atoms in thin metallic foils.

They have a net spin of zero due to the mechanism of their production in standard alpha radioactive decay. The kinetic energy is about 5 MeV and a velocity of 4% in the vicinity of light's speed. Of all the particle radiation, alpha particles are highly ionizing. When associated with radioactive alpha decay, they usually have low penetration power and can be stopped by a few centimeters of the skin or air.

The so-called long-range alpha particles from ternary fission are three times more energetic, and they penetrate three times as far. Helium nuclei form 10-12% of the cosmic rays, and they have higher energy than those produced via the radioactive decay process. Depending on their energy, they may have high penetrating power and can transverse the human body, and penetrate many meters of dense solid shielding. To a lesser extent, this is also true of very high-energy helium nuclei produced by particle accelerators.

Beta Particles

Beta particles are high energy, positrons, or high-speed electrons released from the nucleus by some radionuclides during beta decay. It was discovered by Henri Becquerel while experimenting with fluorescence. He fortuitously found out that uranium exposed a photographic plate, wrapped with black paper, with some unknown radiation that could not be put out like X-rays was noticed.

Beta decay usually takes place in nuclei that have numerous neutrons to achieve stability. Beta decay is of two forms, β− decay and β+ decay, which produce electrons and positrons. Beta particles are also called beta radiation or beta rays. They are more ionizing than gamma rays but less ionizing than alpha particles. The higher the ionizing effect, the greater the damage to living tissue and the lower the radiation's penetrating power.

Beta-particles lose their energy fundamentally by the same process as alpha particles; however, there are distinct vital differences. Because of the masses of the β-particles and orbital electrons, they are similar at non-relativistic velocities. The β-particles can lose a considerable fraction of their energy in a sole collision. The β-particle experiences a wide-angle deflection in such collisions, and consequently, β-particles are ejected out of the beam path all along the length. β-particles have a much greater velocity than alpha particles because their mass is much smaller than the heavy particles' mass.

This more incredible velocity results in an equivalently lower ionization and gives a much longer range to β-particles.

Gamma Rays

A gamma-ray or gamma radiation is a penetrating form of electromagnetic radiation emerging from atomic nuclei's radioactive decay. It comprises the shortest wavelength electromagnetic waves, and so imparts the highest photon energy. Gamma radiation was detected by Paul Villard, a French chemist and physicist, in 1900 while studying the radiation emitted by radium. Ernest Rutherford, in 1903, named these radiation gamma rays based on their relatively strong penetration of matter.

Natural sources of gamma rays emanating on Earth are mainly secondary radiation and radioactive decay from atmospheric interactions with cosmic ray particles. Other rare natural sources, such as terrestrial gamma-ray flashes, produce gamma rays from electron action upon the nucleus. Significant sources of artificial gamma rays include fission, such as that which takes place in high-energy physics experiments, and nuclear reactors, such as nuclear fusion and neutral pion decay.

Traceable to their high penetration power, they can damage internal organs and bone marrow. In contrast to beta and alpha rays, they effortlessly pass through the body. They thus pose a formidable radiation protection challenge, requiring shielding made from dense materials such as concrete or lead. They cannot be reflected off a mirror, and their wavelengths are so small

that they will pass between atoms in a detector. Figure 2.1 shows radioactive

samples that can be used to test detectors.

Figure 2.1: Alpha, Beta and Gamma sources.

Instrumentation

During this research work, various equipment was used in order to achieve success. The equipment used is listed and discussed below.

- Pocket Geiger Radiation Sensor

- Payload box

- Parachute

- SPOT GPS with Lithium Batteries

- Weather balloons

- Helium tank

- STEM at SFA mobile app

- Android phone

- Electrical tape and zip ties

- Packing foam

- Knife and Scissors

- Drop Cloth

- Rubber gloves

- Finderscope or Binoculars

- GoPro camera with memory card and extended battery

- Arduino with SD Shield and 9-Volt Batteries

- Altitude, pressure, temperature, Geiger sensors

Geiger Counter

A Geiger counter is a device that measures and detects ionizing radiation. This invention was named after Hans Geiger, who invented the concept in 1908, and Walther Müller. He worked jointly with Geiger in expanding the technique further in 1928 to bring about a tube counter that could identify several different radiations. It is often used in different applications such as radiation dosimetry, radiological protection, experimental physics, and the nuclear industry. A type 5 Pocket Geiger Radiation Sensor was used for this research. It provides radiation measurements in units of sieverts per unit time.

Pocket Geiger Radiation Sensor

For this research, a type 5 Pocket Geiger Radiation Sensor was purchased from Sparkfun. This Geiger counter is an extremely sensitive radiation sensor manufactured and designed for the nested systems market. It effectively detects Gamma and Beta radiation. This sensor has a simple pulsed output that can be used with any microcontroller. These Geiger counters can feature a measurement range of 0.05 µSv/h (microsieverts per hour) to 10 mSv/h (millisievert per hour) at 0.01 cpm (counts per minute) to 300 Kcpm with a required measurement time of two minutes. The Pocket Geiger has an onboard DC boost circuit so that the board can be supplied with a 3 V to 9 V. Figure 2.2 shows an image of the Type-5 Pocket Geiger Radiation Sensor used in this research.
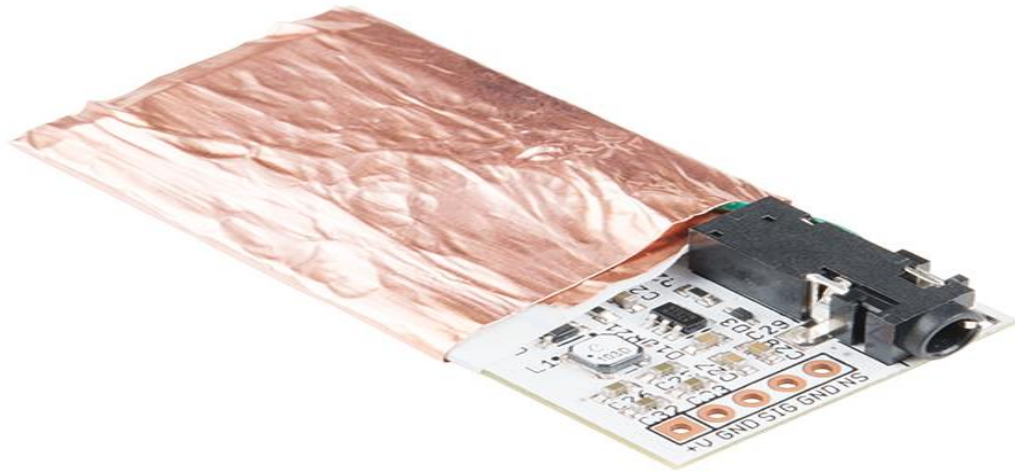
Figure 2.2: Type-5 Pocket Geiger Radiation Sensor.

Board Pins

They are machined individual pins used for various plug-in applications and functionally the dynamic building blocks within the interconnect system, known as printed circuit board (PCB) pins. Figure 2.3 shows the pins that were soldered to components in this research.

Figure 2.3: Board pins used for component connections.

The payload box was loaded with an Android phone, breadboard, Geiger counter, ESP32 (Arduino with SD shield), purple power bank, SPOT GPS, business card, and packing foam. Each of the components were glued to the box to prevent movement while in flight. Contact details were placed in the box in the event that the payload was found. Packing foam was placed in the box to further prevent the components from getting out of place while in flight. The phone in the payload box serves as the transmitter of the data while the payload was in flight. With all the components arranged inside the payload box, the foam was placed over the components and the lid of the box was closed. The payload box was then fastened to the parachute and electrical tape was used to support the ropes that fasten the payload to the parachute. Figures 2.4 through 2.6 show view of the payload.

Figure 2.4: The components before it was loaded into the payload box.

Figure 2.5: The components after it was loaded into the payload box.
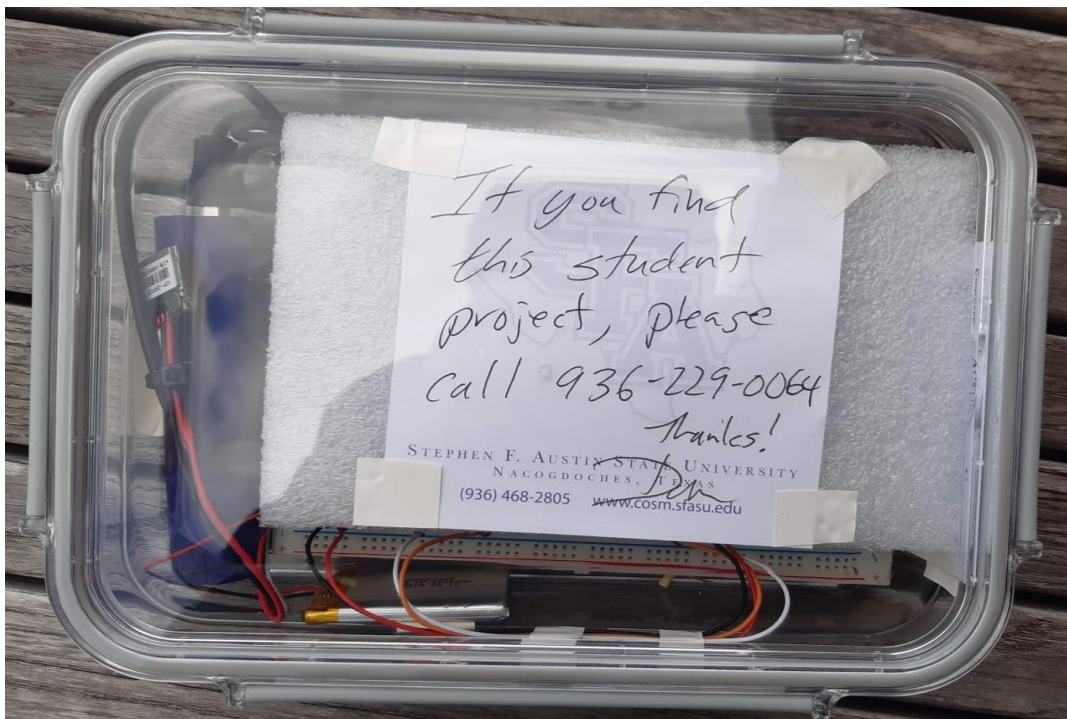
Figure 2.6: The components loaded and secured with the foam and lid.

Parachute

When carrying out a high altitude weather balloon project, the balloon rises into the atmosphere and the balloon expands due to lower pressure. When certain altitudes are reached, the balloon bursts and parachutes back to the ground. The payload parachute is what slows the payload down for a soft and safe landing. Figures 2.7 and 2.8 shows the images of the payload attached to the parachute and payload secured by the electrical tape respectively.

Figure 2.7: The payload attached to the parachute.
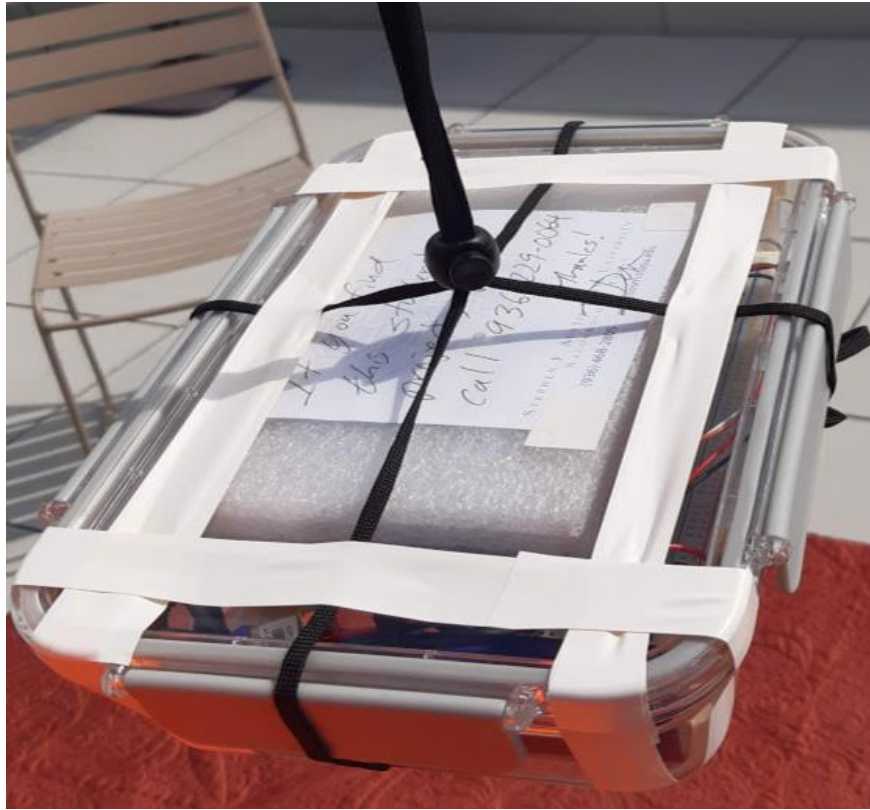
Figure 2.8: The payload fastened to the parachute with electrical tape.

Helium Balloon

The weather balloon used in this project was model #8240 from Scientific Sales, Inc. Helium was used to fill the weather balloon because it is lighter than air. The balloon's mass was 0.60 kg before it was filled with Helium while the mass of the payload with parachute was 0.96 kg giving a total mass of 1.56 kg.

Archimedes principle can be used to find the volume of helium needed to lift the balloon. From that we can determine the diameter of the balloon required for the experiment. We begin with Newton's Second law and assume a constant assent rate. F_g is the weight of the experiment and F_b is the buoyant force.

$$\sum F = ma \dots\dots\dots\dots\dots\dots\dots\dots\dots\dots\dots\dots\dots\dots\dots\dots\dots(1)$$

$$F_b - F_g = 0 \dots\dots\dots\dots\dots\dots\dots\dots\dots\dots\dots\dots\dots\dots\dots(2)$$

$$m_{air}g - m_{payload}g - m_{He}g = 0 \dots\dots\dots\dots\dots\dots\dots\dots\dots(3)$$

$$m_{air} - m_{payload} - m_{He} = 0 \dots\dots\dots\dots\dots\dots\dots\dots\dots\dots(4)$$

$$m_{payload} = m_{air} - m_{He} \dots\dots\dots\dots\dots\dots\dots\dots\dots\dots\dots(5)$$

$$m_{payload} = (\rho_{air} - \rho_{He})V \dots\dots\dots\dots\dots\dots\dots\dots\dots\dots\dots(6)$$

$$V = \frac{m_{payload}}{(\rho_{air} - \rho_{He})} \dots\dots\dots\dots\dots\dots\dots\dots\dots\dots\dots\dots\dots(7)$$

The values needed to calculate the volume are as follows:

$$m_{payload} = 1.56kg \qquad \rho_{air} = 1.2\ kg/m^3 \qquad \rho_{He} = 0.164\ kg/m^3$$

Therefore,

$$V = \frac{1.56\ kg}{(1.2\ kg/m^3 - 0.164\ kg/m^3)}$$

$$V \ = \ 1.51 \, m^3$$

From the volume of the balloon, the diameter of the balloon can be estimated using:

$$V = \frac{4}{3}\pi r^3 \dots\dots\dots\dots\dots\dots\dots\dots\dots\dots\dots\dots\dots\dots\dots\dots\dots(8)$$

$$V \ = \frac{4}{3} \ \pi \left(\frac{d^3}{2}\right) \ \dots\dots\dots\dots\dots\dots\dots\dots\dots\dots\dots\dots\dots\dots(9)$$

$$V \ = \frac{4}{24}\pi d^3 \ \dots\dots\dots\dots\dots\dots\dots\dots\dots\dots\dots\dots\dots\dots\dots\dots(10)$$

$$V \ = \frac{1}{6}\pi d^3 \dots\dots\dots\dots\dots\dots\dots\dots\dots\dots\dots\dots\dots\dots\dots\dots(11)$$

The result is then:

$$d \ = \ \sqrt[3]{\frac{6V}{\pi}}$$

$$d \ = \ \sqrt[3]{\frac{6(1.511 \, m^3)}{\pi}}$$

$$d \ = \ 1.42 \, m.$$

Therefore, for this experiment the balloon should be filled with helium until its diameter is more than 1.42 meters. Figure 2.9 shows the size of the balloon.

Figure 2.9 Size of the weather balloon.

<u>SPOT GPS</u>

SPOT GPS is a low-budget satellite safety device, delivering reliable location-based tracking. For the purpose of the near space launch the SPOT GPS was used to monitor the location of the payload while in flight. For the SPOT GPS to report live locations, the device was registered on the FindMeSpot.com website and the device was registered as "Red1". For the device to be turned three lithium batteries were inserted. The SPOT GPS live location could be viewed online. The SPOT GPS was fastened to the top of the payload using a cable tie. The SPOT GPS reported that the payload landed at 04:52 PM at Jewel Hill Road, Waller Landing, in Northeast Louisiana, with a longitude and latitude of 32.05360°N and 91.60956°W respectively at a

horizontal speed of 0.02 mph. The data during the time of flight was extracted

from the online monitoring database. Figure 2.10 and 2.11 shows the image of

the SPOT GPS and SPOT GPS with Lithium batteries respectively.

Figure 2.10: SPOT GPS.

Figure 2.11: SPOT GPS with Lithium batteries.

Android Phone

The android phone was used as a data transmitter while the payload was in flight. The android phone receives the data from the Arduino device and transmits it to the database on Google Drive. Figure 2.12 and 2.13 shows the screenshot from the Android app called Serial Bluetooth Terminal before flight and screenshot showing the process of data collection respectively.

```
10:15:26.740 1.06+/-0.03
10:15:28.663 1.06+/-0.03
10:15:28.815 1.07+/-0.03
10:15:29.607 1.07+/-0.03
10:15:29.784 1.07+/-0.03
10:15:29.945 1.07+/-0.03
10:15:30.458 $GPRMC,161522.00,A,3137.11140,N,
09438.92745,W,0.025,,110321,,,A*6E
10:15:30.459
10:15:31.688 1.07+/-0.03
10:15:32.175 1.08+/-0.03
10:15:33.288 1.08+/-0.03
10:15:34.586 1.08+/-0.03
10:15:36.975 1.07+/-0.03
10:15:38.106 1.07+/-0.03
10:15:39.714 1.07+/-0.03
10:15:40.459 $GPRMC,161532.00,A,3137.11152,N,
09438.92665,W,0.076,,110321,,,A*69
10:15:40.472
10:15:40.826 1.07+/-0.03
10:15:41.929 1.07+/-0.03
10:15:42.413 1.06+/-0.03
10:15:43.847 1.06+/-0.03
10:15:44.653 1.07+/-0.03
10:15:44.817 1.07+/-0.03
```

Figure 2.12: Screenshot from data phone before flight.
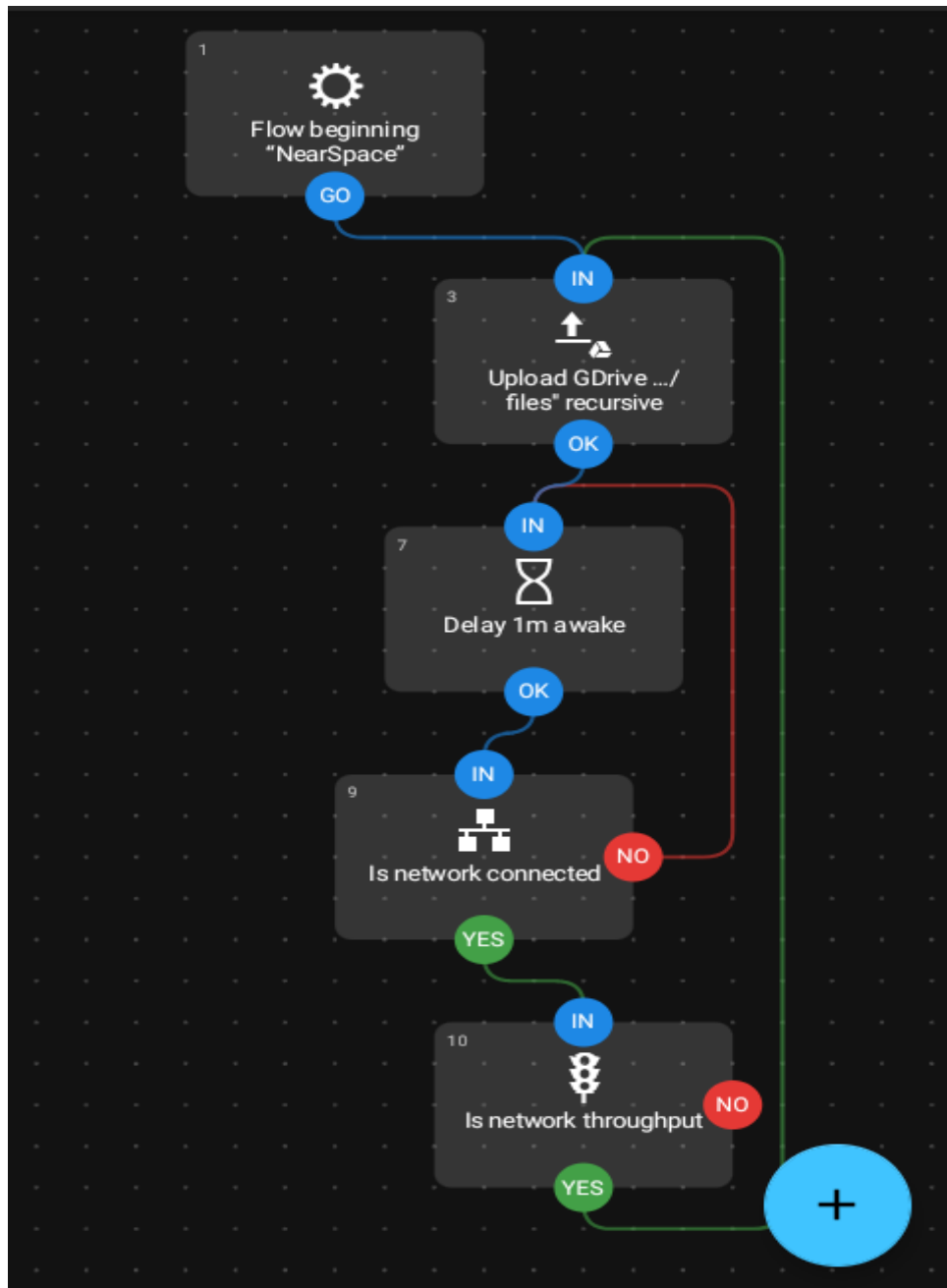
Figure 2.13: Screenshot showing the process of data collection using the Android app called *Automation*.

Circuit Construction

The Pocket Geiger Radiation Sensor and the ESP32 Thing (Arduino) were connected to a breadboard using jumper wires. Four pieces of 1mm board pins were placed directly onto the top and soldered to the bottom firmly onto the circuit board. Then five pieces of Arduino jumper wires were inserted over the soldered board pin. The five pins had different colors for easy identification. The red jumper cable connected to +V, the black jumper cable to GND (ground), the orange jumper cable to SIG (signal), the fourth pin was left unused, and the brown jumper cable to NS (noise). The Pocket Geiger Radiation Sensor was then connected to the breadboard using jumper cables. A buzzer was placed on the breadboard across the "e-f" section. A 330 Ω resistor was placed in series at holes 13 through 19 (labeled 'i' on the schematic). Two jumper cables were pinned into hole 29 (labeled 'h-i' on the schematic) and then connected to the GND on the Arduino device into hole 12 (labelled 'i' on the schematic respectively).

A single jumper cable was pinned into hole 29 (labelled 'c' on the schematic) and then the other end was then pinned into port 8 on the digital pulse width modulation (PWM) of the Arduino device. Two jumper cables were pinned into the digital (PWM) of the Arduino device at pin 2 and 3 of the schematics at hole 20 through 21 (labelled "a" on the schematic). Two jumper cables from the power section of the Arduino device labelled GND and 5V were pinned to the breadboard into hole 22 through 23 (labelled 'a' on schematic). The led light was pinned across the schematics (labelled 'd' through 'g') and

then the four jumper cables from the Pocket Geiger Radiation Sensor were pinned into hole 20 through 23 (labelled 'a').

Figure 2.14 through 2.19 shows the top and bottom view of the soldered circuit board, Arduino jumper pins connection, circuit diagram, Arduino circuit connections and the cabling of the Pocket Geiger Radiation Sensor with the Arduino device and breadboard respectively.
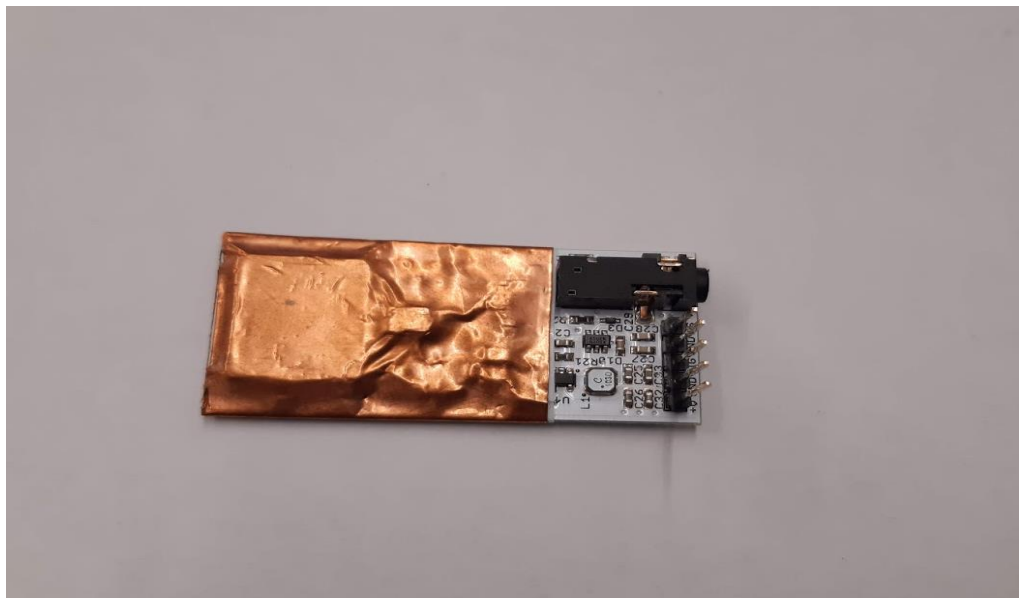
Figure 2.14: Top view of the board pins soldered to the circuit board of the Pocket Geiger Radiation Sensor.
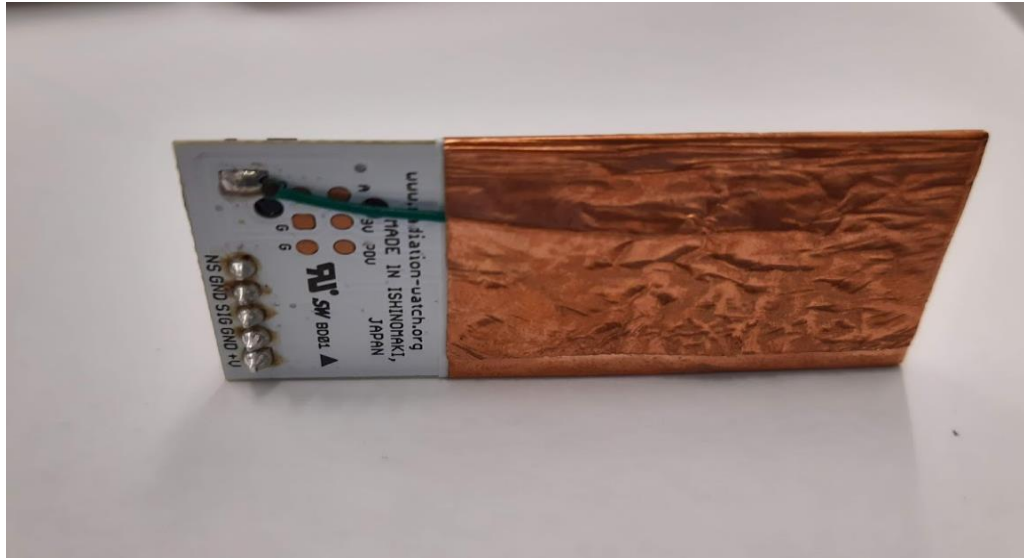
Figure 2.15: Bottom view of the board pins soldered to the circuit board of the

Pocket Geiger Radiation Sensor.
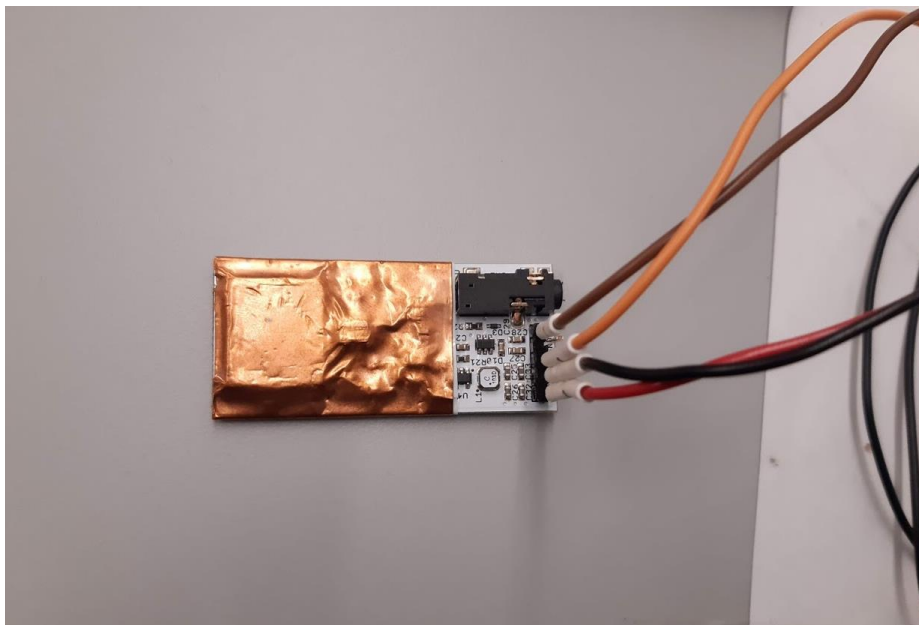
Figure 2.16: The Arduino jumper wires pinned to the board pins on the Pocket

Geiger Radiation Sensor.
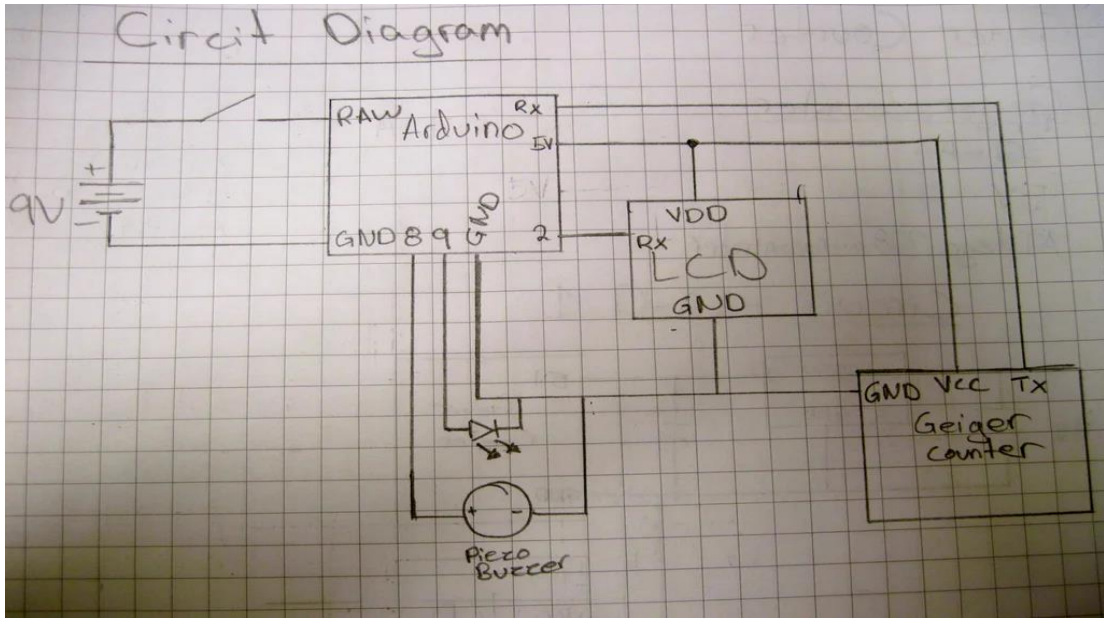
Figure 2.17: The circuit sketch for the set up.
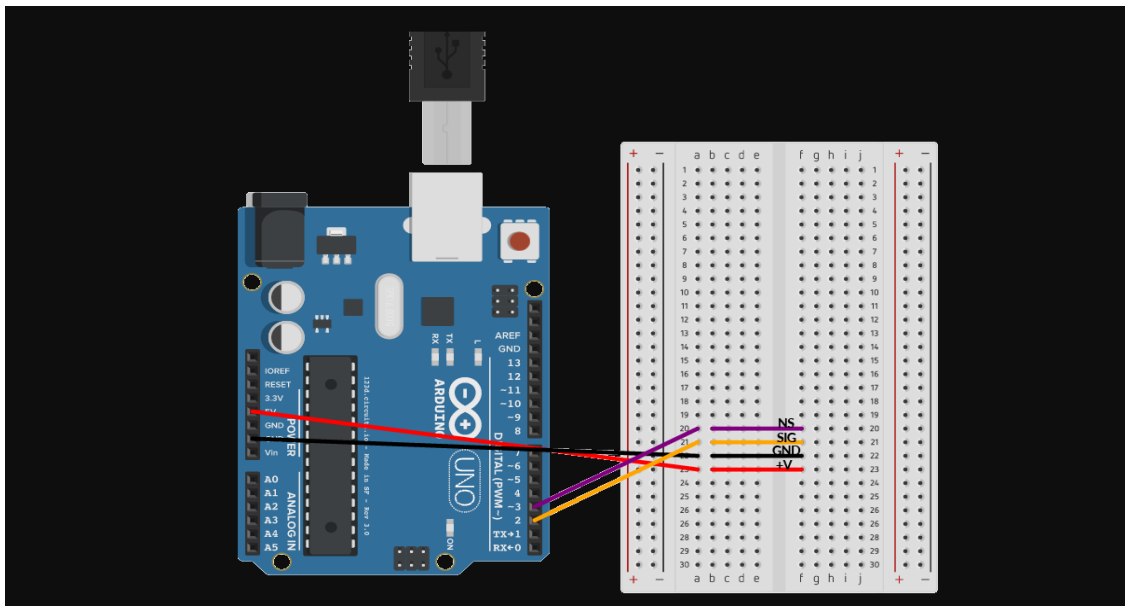
Figure 2.18: An illustration of how the Arduino is connected with the

breadboard.
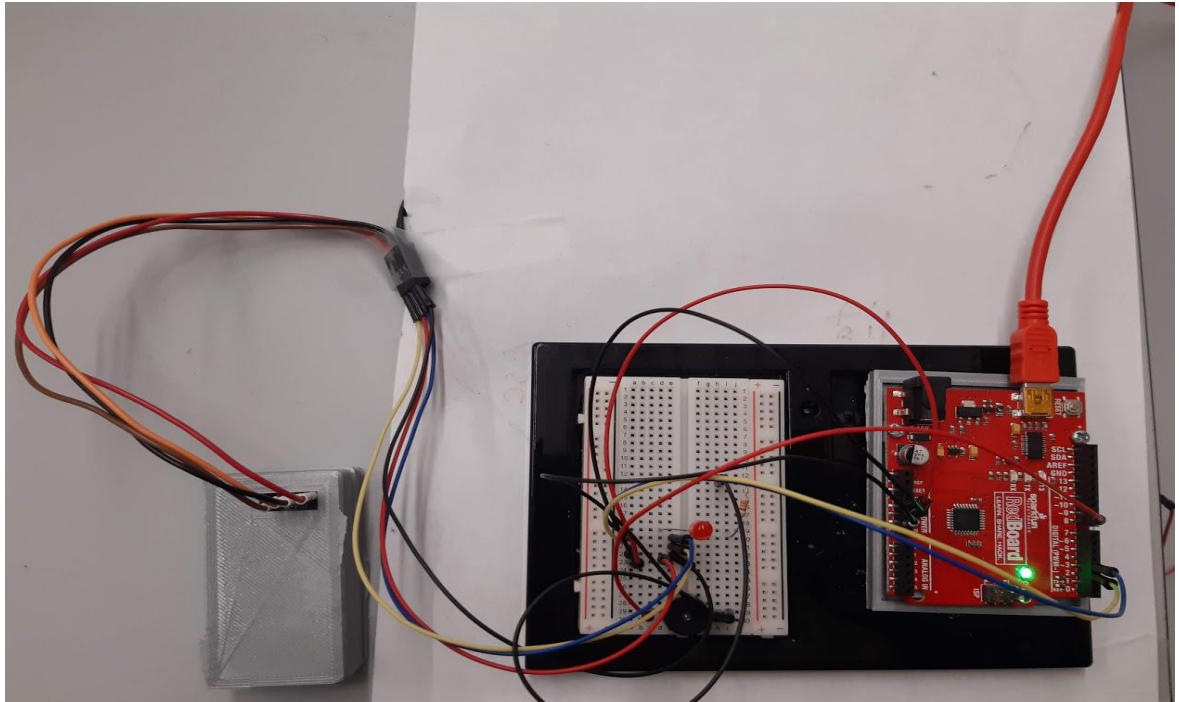
Figure 2.19: Cabling of the Pocket Geiger Radiation Sensor with the Arduino

device and breadboard.

Arduino Code

The code was written using the Arduino Software (IDE) v1.8.13, and the code was then uploaded onto the Arduino device with a USB connection to the computer's CPU. The data output was then displayed on the monitor via the Arduino 1.8.13 application.

CODE

```
# SFA-NearSpace-Geiger-Bluetooth-GPS.ino

#include "RadiationWatch.h"

/*

This example works as the SimpleSerialPrinter, except it

also generates tick noise for each radiation hitting the

Pocket Geiger.

You need a piezo buzzer or similar connected to pin 8.

*/

#include "BluetoothSerial.h"

#if !defined(CONFIG_BT_ENABLED) ||

!defined(CONFIG_BLUEDROID_ENABLED)

#error Bluetooth is not enabled! Please run `make

menuconfig` to and enable it

#endif

BluetoothSerial SerialBT;

#include <Arduino.h>

HardwareSerial GPSUART(2);

#define PRINT_SPEED 10000 // 250 ms between prints

#define AUX_LED_PIN 13

#define ESP_LED_PIN 5

static unsigned long lastPrint = 0; //print time

RadiationWatch radiationWatch;
```

```
void onRadiation(){

  //Output classic geiger counter tick noise.

  //tone(PIN_TONE, 800, 1);

  Serial.println("A wild gamma ray appeared");

  Serial.print(radiationWatch.uSvh());

  Serial.print(" uSv/h +/- ");

  Serial.println(radiationWatch.uSvhError());

  SerialBT.print(radiationWatch.uSvh());

  SerialBT.print("+/-");

  SerialBT.println(radiationWatch.uSvhError());

  delay(20);

}

void onNoise(){

  Serial.println("Argh, noise, please stop moving");

}

void setup(){

  Serial.begin(9600);

  GPSUART.begin(9600);

  delay(1000);

  Serial.println("Sketch Started.");

  SerialBT.begin("ESP32test"); //Bluetooth device name

  Serial.println("The device started, now you can pair it

with bluetooth!");
```

```
    radiationWatch.setup();

    // Register the callbacks.

    radiationWatch.registerRadiationCallback(&onRadiation);

    radiationWatch.registerNoiseCallback(&onNoise);


}

int parsingState = 0;

char parseBuffer[200];

int parseBufferPtr = 0;

void loop() {

    radiationWatch.loop();

    //Pass GPS data to the SD card

    switch(parsingState) {

        case 0: //reset buffer

            parseBuffer[0] = '$';

            parseBufferPtr = 1;

            parsingState = 1;

        break;

        case 1:

            if(GPSUART.available()) {

                char c = GPSUART.read();

                if(c == '$') {

                    //detected end
```

```
parseBuffer[parseBufferPtr] = 0;

parseBufferPtr++;

//Pick out good messsage

if(( parseBuffer[1] == 'G')&&( parseBuffer[2] ==

'P')&&( parseBuffer[3] == 'R')&&( parseBuffer[4] ==

'M')&&( parseBuffer[5] == 'C')) {

Serial.write(parseBuffer);

if ((lastPrint + PRINT_SPEED) < millis()) {

  SerialBT.println(parseBuffer);

  lastPrint = millis(); // Update lastPrint time

}

//Output data to terminal for debug

//Serial.print(parseBuffer);

digitalWrite(AUX_LED_PIN, 1);

delay(1);

int seekPtr = 0;

while((parseBuffer[seekPtr] != ',')

   &&(seekPtr < 25)) {

      seekPtr++;

}

seekPtr++;

while((parseBuffer[seekPtr] != ',')

   &&(seekPtr < 25)) {
```

```
                        seekPtr++;

            }

        seekPtr++;

        if(parseBuffer[seekPtr] == 'A') {

                //digitalWrite(AUX_LED_PIN, 1);

            } else {

                digitalWrite(AUX_LED_PIN, 0);

            }

        }

        parsingState = 0;

    } else {

        parseBuffer[parseBufferPtr] = c;

        parseBufferPtr++;

    }

    }

    break;

    default:

    break;

    }

}
```

CHAPTER THREE

OBSERVATION AND ANALYSIS

Bench Test with Radioactive Sources

       The aim of the bench test is to verify the correctness of the connection of the Pocket Geiger Radiation Sensor, the breadboard, and the Arduino board using different radiation sources. The bench test was conducted in the laboratory using the Geiger Counter, radiation sources such as Strontium-90 for the beta source, Polonium-210 for the alpha source, and Cobalt-60 for the gamma source. The sources were individually placed at different distances on a retort stand above the Pocket Geiger Radiation Sensor. The distance was correctly measured using a ruler in centimeters starting from 0 cm to 14cm. The Pocket Geiger Counter was connected to a breadboard and the Arduino circuit board.

Bench Test Result for Polonium-210

       The radioactive sample Polonium-210 is a source of alpha particles. Polonium-210 was placed at a different distance (0 cm to 14 cm) above the Pocket Geiger Radiation Sensor. The Geiger counter could not detect the alpha source because of the shielding on the counter; therefore, it was determined that the Geiger counter was only going to be useful for other types of radiation.

Bench Test Result for Strontium-90

The radioactive sample Strontium-90 is a source of beta particles. Strontium-90 was placed at a different distance (0 cm to 14 cm) above the Pocket Geiger Radiation Sensor. The resulting data count per minute (CPM) is inversely proportional to the height in centimeters. As height from the source increases, the count per minute decreases as shown in Table 3.1 and Figure 3.1.

Table 3.1: Resulting data from Strontium-90 (beta source).

Height (cm)	CPM
0	376
1	300
2	295
3	280
4	177.11
5	148.03
6	129.65
7	98
8	91.76
9	69.79
10	53.16
11	54.71
12	46.17
13	45.9
14	31

The plot of CPM vs. Height (cm) for Stronium-90
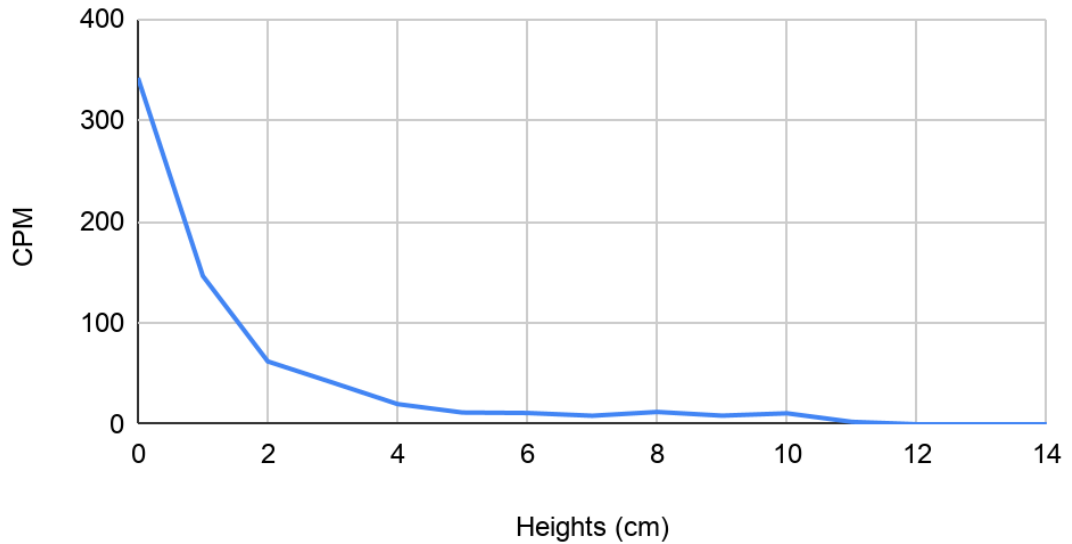
Figure 3.1: The plot of CPM versus height for Strontium-90 (Beta source).

Bench Test Result for Cobalt-60

The radioactive sample Cobalt-60 is a source of gamma rays. Cobalt-60 was placed at a different distance (0 cm to 14 cm) above the Pocket Geiger Radiation Sensor. The resulting data count per minute (CPM) is inversely proportional to the height in centimeters. As height from the source increases, the count per minute decreases as shown in Table 3.2 and Figure 3.2.

Table 3.2: Result from bench test for Cobalt-60.

Heights (cm)	CPM
0	341.79
1	146.27
2	62
3	41.1
4	19.89
5	11.57
6	11.11
7	8.4
8	12.13
9	8.48
10	10.79
11	2.36
12	0
13	0
14	0

The plot of CPM vs. Height(cm) for Co-60
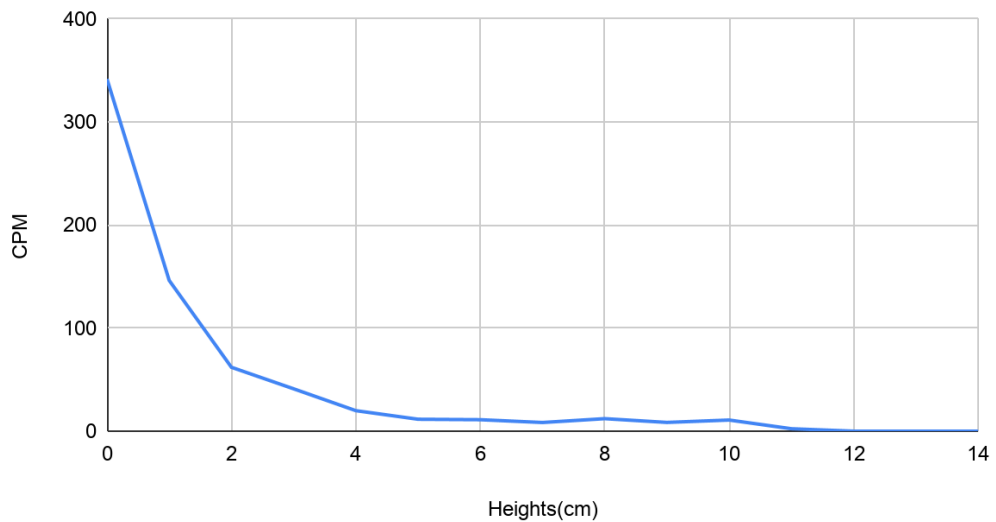
Figure 3.2: The plot of CPM versus height for Cobalt-60 (Gamma source).
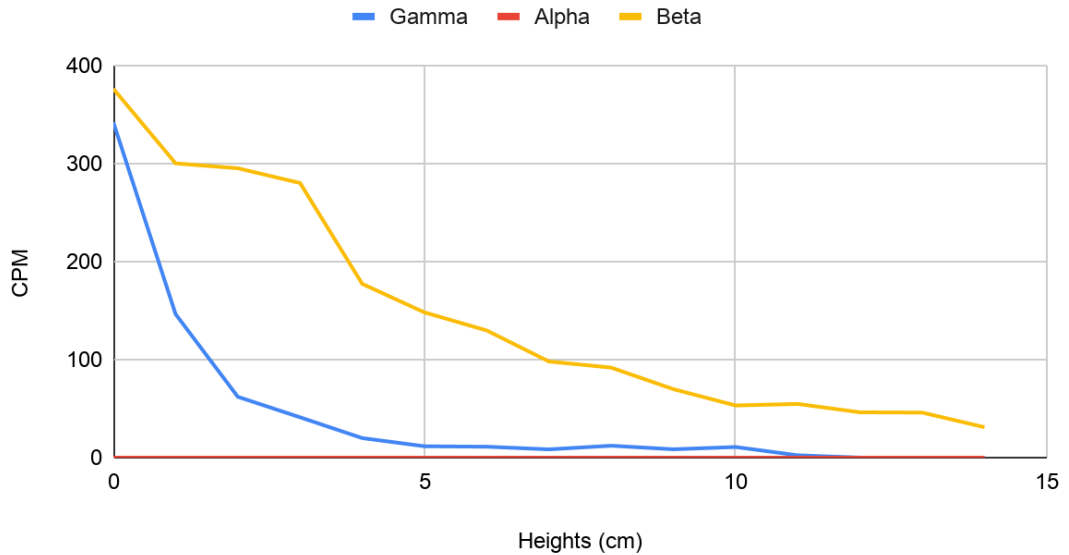
Figure 3.3: The comprehensive plot of CPM versus height for each sources.

<u>Bench Test Conclusions</u>

In conclusion, the detector is capable of detecting only gamma and beta radiation. Also, it is most sensitive to beta radiation. To determine the accuracy of the bench test, the signal-to-noise ratio was evaluated. The signal-to-noise ratio is defined as the ratio between the desired information or the power of a signal and the background noise power. Using this formula,

$$SNR \ = \ S - N$$…………………………..(1)

Every time we deal with a source of particles arriving randomly, the noise associated with that randomness is

$$N \ = sqrt(\, n)$$……………………………………(2)

where n is the number of particles. This means that the percent error (error bars) for the CPM versus height graph would be as follows:

$$Percent\ Error\ =\ (100\%\ *\ sqrt(n))/n…………(3)$$

The Pocket Geiger Radiation Sensor uses this estimate to provide a range of uncertainty in the radiation levels (e.g. +/- 1 µSv/h).

Payload Drop Test

On the 9th of March 2021, a payload drop test was carried out on the observation deck of the Ed & Gwen Cole STEM Building on the SFA campus with a temperature of 75°F. The payload was attached to a parachute and within the payload box was an android phone and packing foam. The foam acted as a shock absorber against impact when the payload hit an obstacle. Before the payload was dropped, the *STEM at SFA* mobile app was installed on the phone. The *STEM at SFA* mobile app has an acceleration module that can record acceleration at various rates. The period of measurement was set at 25 milliseconds for 45 seconds. The payload was dropped from the observation deck to the ground. The data recorded from the acceleration module was then exported and then analyzed. Figure 3.4 shows the interface of the STEM at SFA mobile app used to record acceleration module for drop tests.
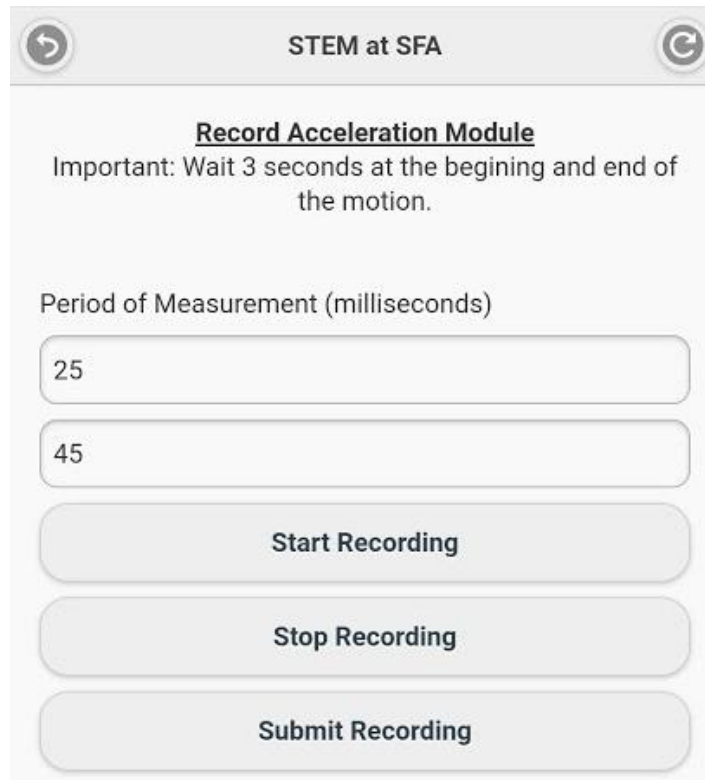
Figure 3.4: The interface of the STEM at SFA mobile app used to

record acceleration module for drop test.

Analysis of the Data from the Drop Test

Table 3.3 shows the result of the acceleration during the drop test of the payload with the parachute. From Figure 3.6 the free fall time is approximately 28.1 seconds - 24.0 seconds = 4.1 seconds. The distance of the fall was 16.0 meters. Therefore, assuming a constant speed the terminal velocity is about 3.90 m/s. This estimate can be used in modeling the flight path of the payload.

Table 3.3: Acceleration module result for drop test.

Time (m/s)	a_x (m/s^2)	a_y (m/s^2)	a_z (m/s^2)
29.98168945	-0.056	0.156	9.794
49.87182617	-0.117	0.147	9.812
79.90893555	-0.156	0.131	9.762
99.85620117	-0.182	0.151	9.849
129.7990723	-0.141	0.15	9.824
159.7888184	-0.113	0.142	9.831
179.7390137	-0.128	0.169	9.827
209.7050781	-0.206	0.13	9.816
239.6369629	-0.114	0.143	9.777
259.5849609	-0.049	0.158	9.776
289.6450195	-0.189	0.141	9.856
309.5646973	-0.194	0.141	9.823
339.5310059	-0.117	0.154	9.797
369.46875	-0.139	0.129	9.805
389.4108887	-0.142	0.153	9.808
419.3339844	-0.172	0.149	9.823
449.1369629	-0.159	0.159	9.83
469.2868652	-0.119	0.185	9.804
499.0917969	-0.155	0.12	9.794
519.1359863	-0.175	0.152	9.824
549.1140137	-0.116	0.15	9.813
578.9567871	-0.191	0.142	9.85
598.8898926	-0.135	0.15	9.821
628.817627	-0.131	0.166	9.813
648.9716797	-0.169	0.141	9.788
678.7509766	-0.123	0.16	9.807
708.8310547	-0.14	0.15	9.755
728.6679688	-0.174	0.094	9.86
758.6318359	-0.126	0.188	9.881
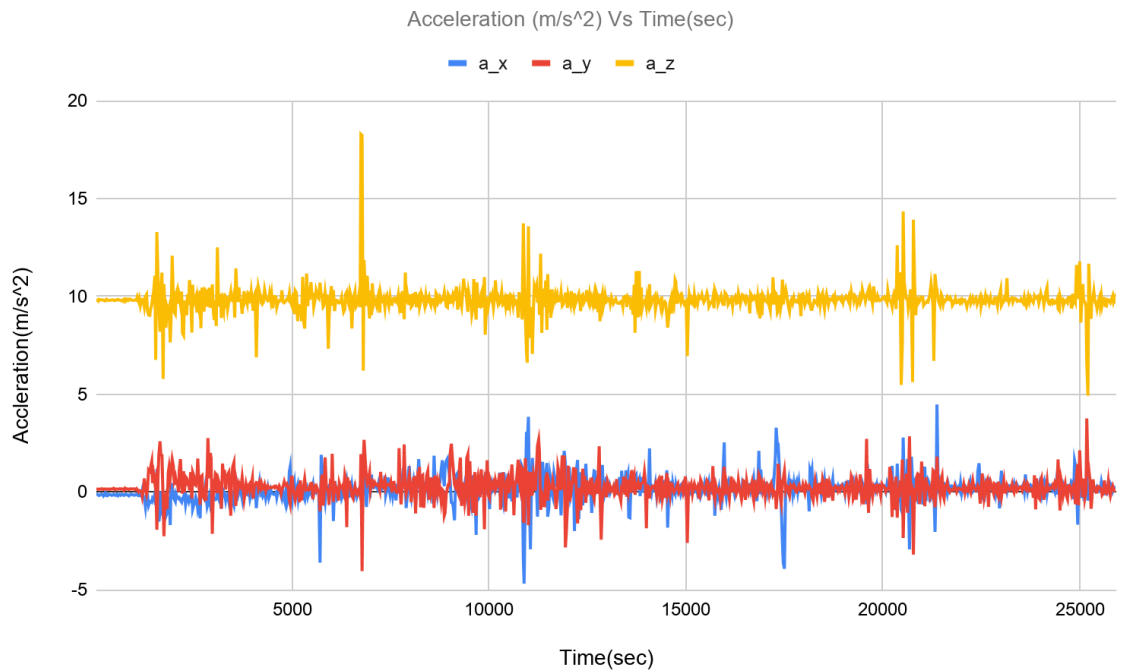
Figure 3.5: The plot of acceleration versus time.
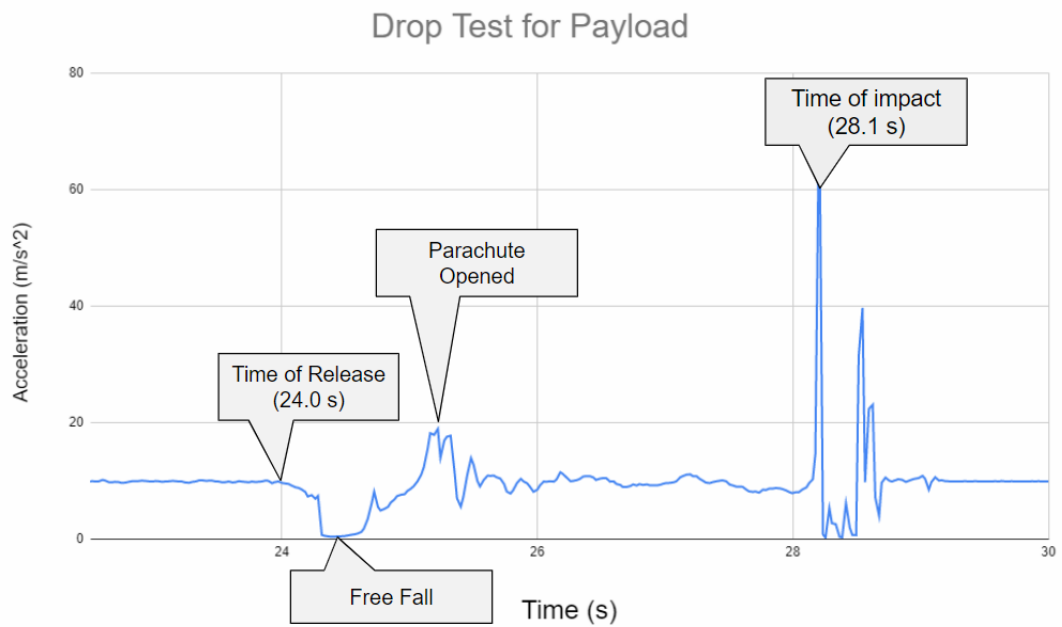
Figure 3.6: The drop test for payload.

<u>Pre-Launch Preparation</u>

Preparing for the Near Space launch took five days of continuous work, which started on March, 8 2021, with hanging off the parachute and checking the connection points. The circuit and code were thoroughly checked and tested for possible failures. The mass of the payload components were measured and recorded. The forecast was checked ahead for the proposed launch day, which was planned for Thursday, March 11, 2021 by 10 am. Figure 3.48 and 3.49 shows the prototype of the weather balloon to be launched and the actual weather balloon launched respectively.
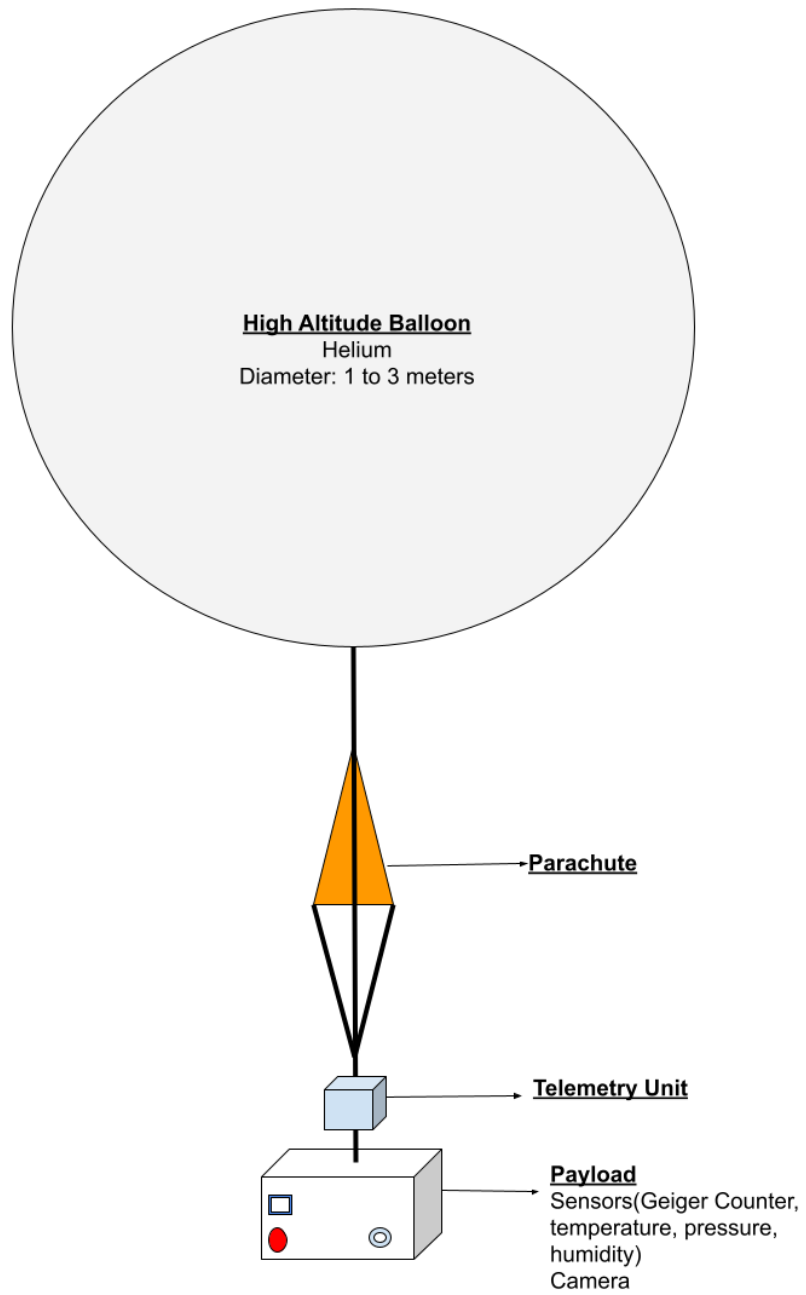
Figure 3.7: The prototype of the weather balloon launched.
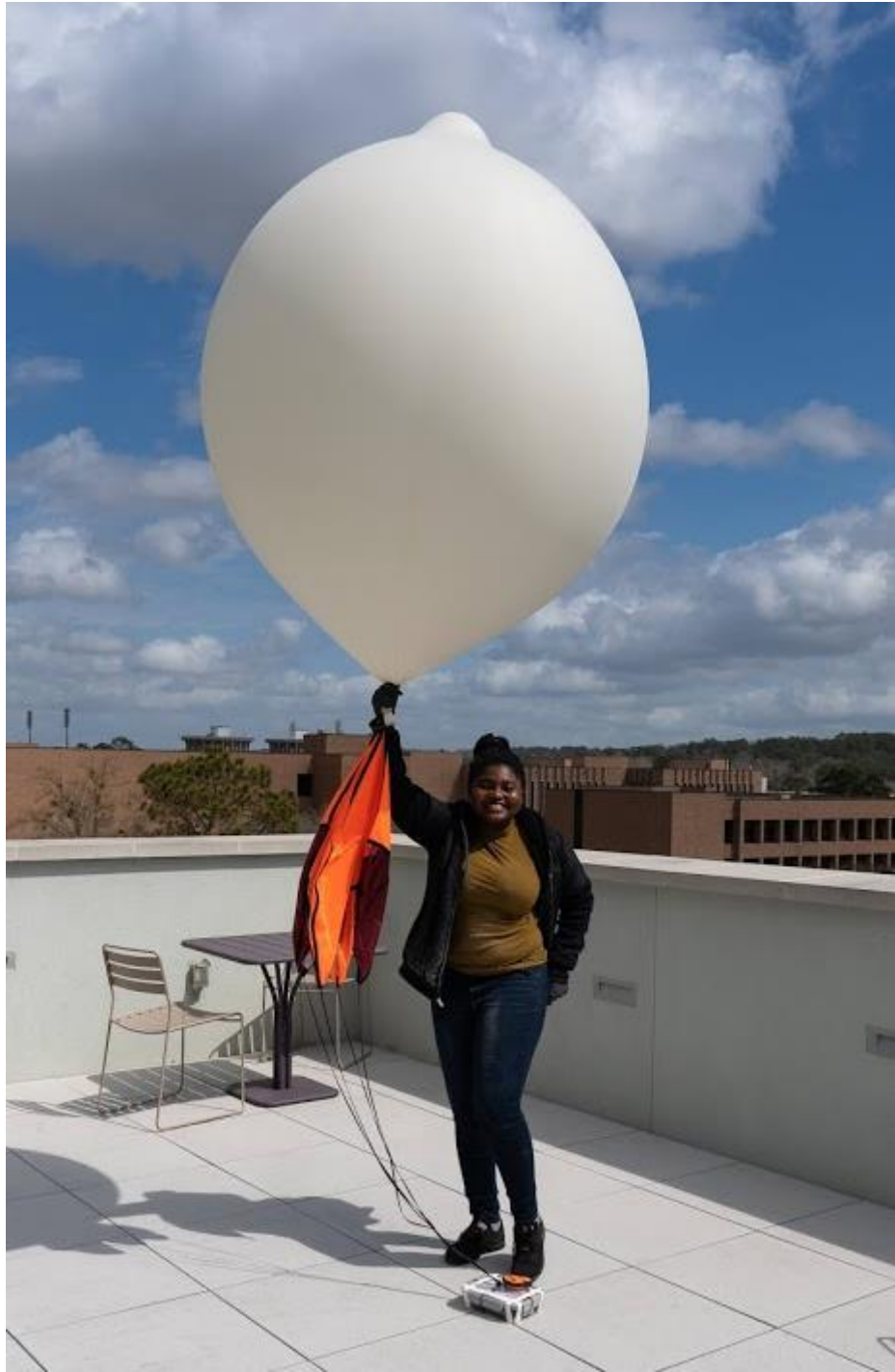
Figure 3.8: The actual weather balloon launched

Prediction of the Flight Path

The Cambridge University Spaceflight landing predictor was used to predict the flight of travel and the landing location of the weather balloon and the bayload. This prediction tool is available at predict.habhub.org (UK High Altitude Society, 2021). The longitude and latitude of the launching location (31.6194881° ,-94.6497343° respectively) were entered on the interface along with the launch altitude of 92m. A launch time was chosen for 10:00 AM which is 16:00 UTC. The launch date was entered as March 11, 2021. The ascent rate was estimated to be 5 m/s with a burst altitude ranging from 3000 meters to 30,000 meters. This range of burst altitudes is equivalent to 10,000 ft to 100,000 ft or 1.9 miles to 19 miles. The descent rate was also estimated to be 5 m/s after verifying from the data resulting from the drop test carried out on March 9, 2021.

The range in kilometers and the flight time were determined via the prediction tool for each burst altitude from 3000 m to 30,000 m, the resulting data was tabulated and analysed. From the prediction of path the payload is estimated to land within Campti, Texas for a burst altitude of 30,000 m.
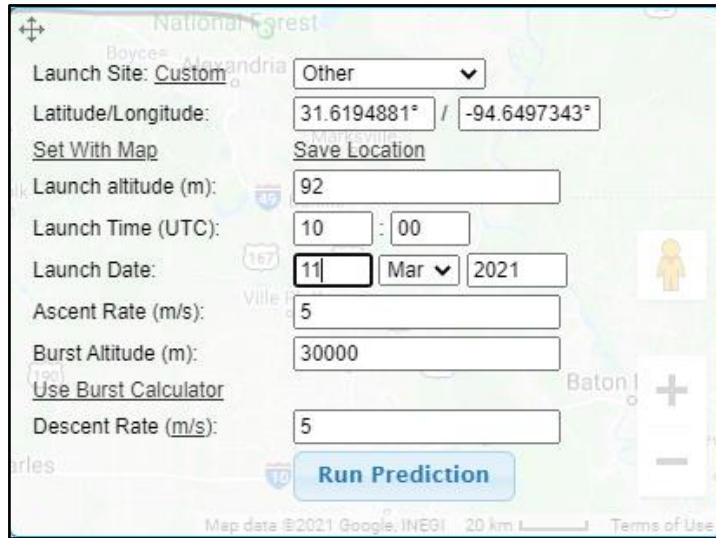
Figure 3.9: Shows the interface to enter the parameters to run prediction.
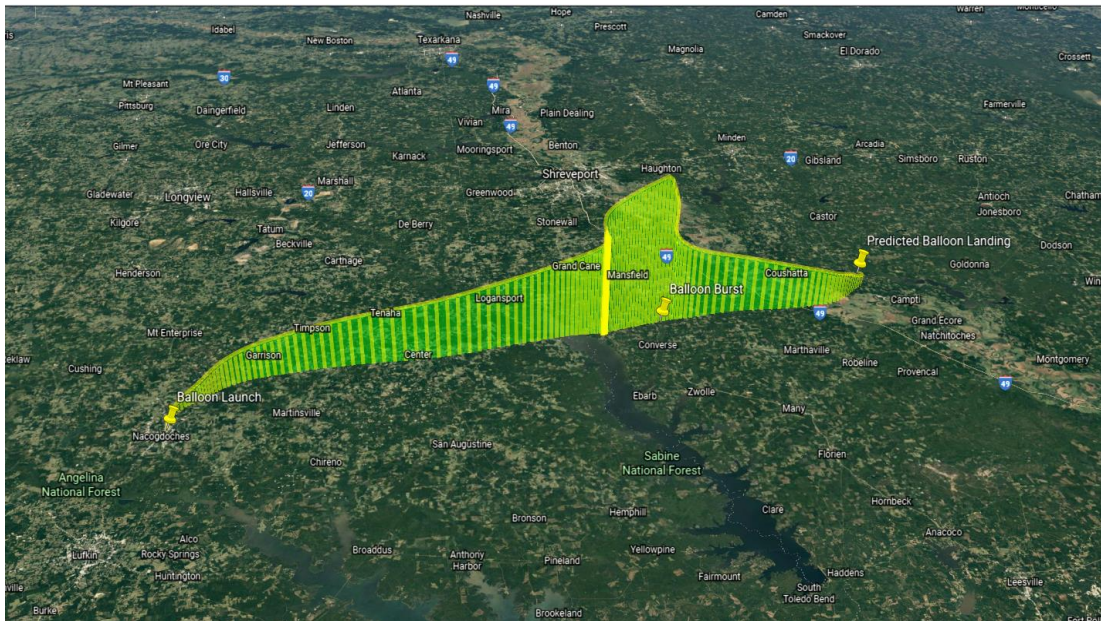
Figure 3.10: The satellite image of the predicted path.
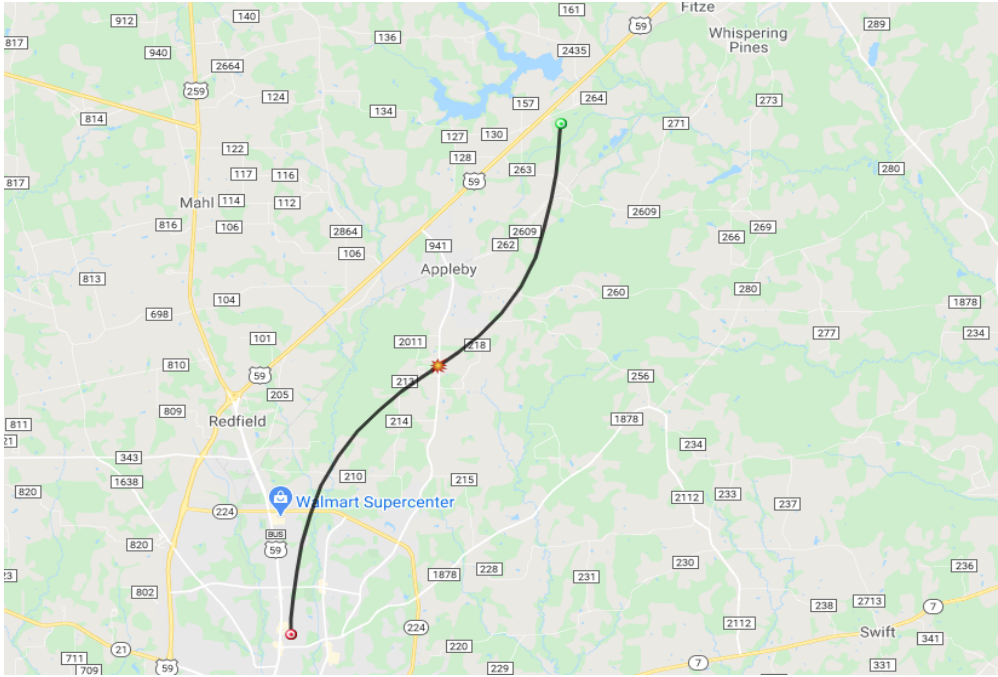
Figure 3.11: The predicted path if the burst altitude was 3000 m.
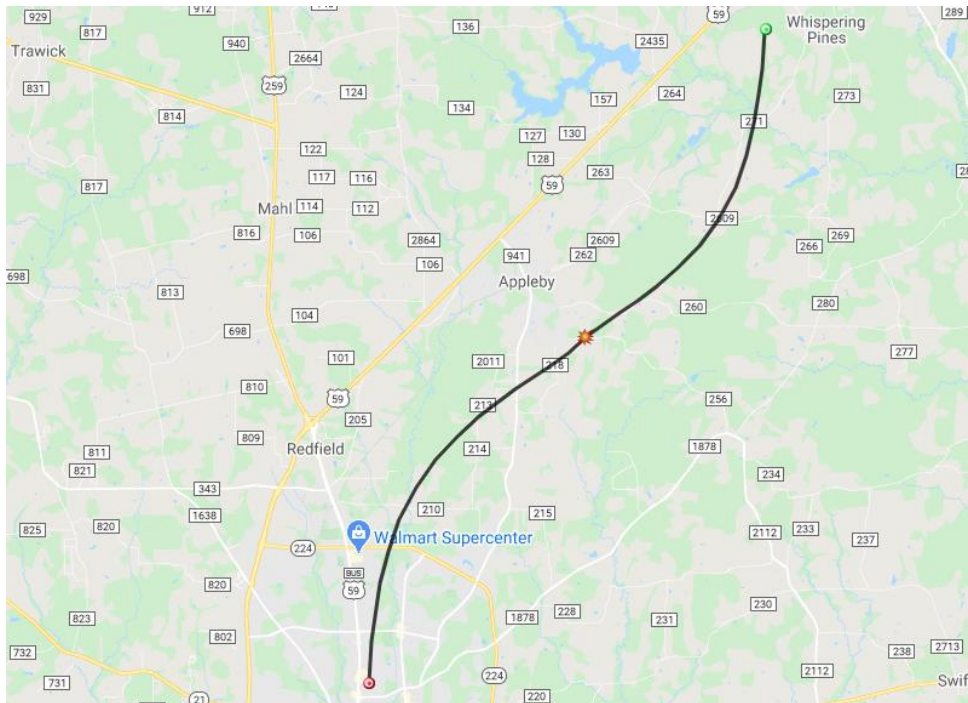
Figure 3.12: The predicted path if the burst altitude was 4000 m.
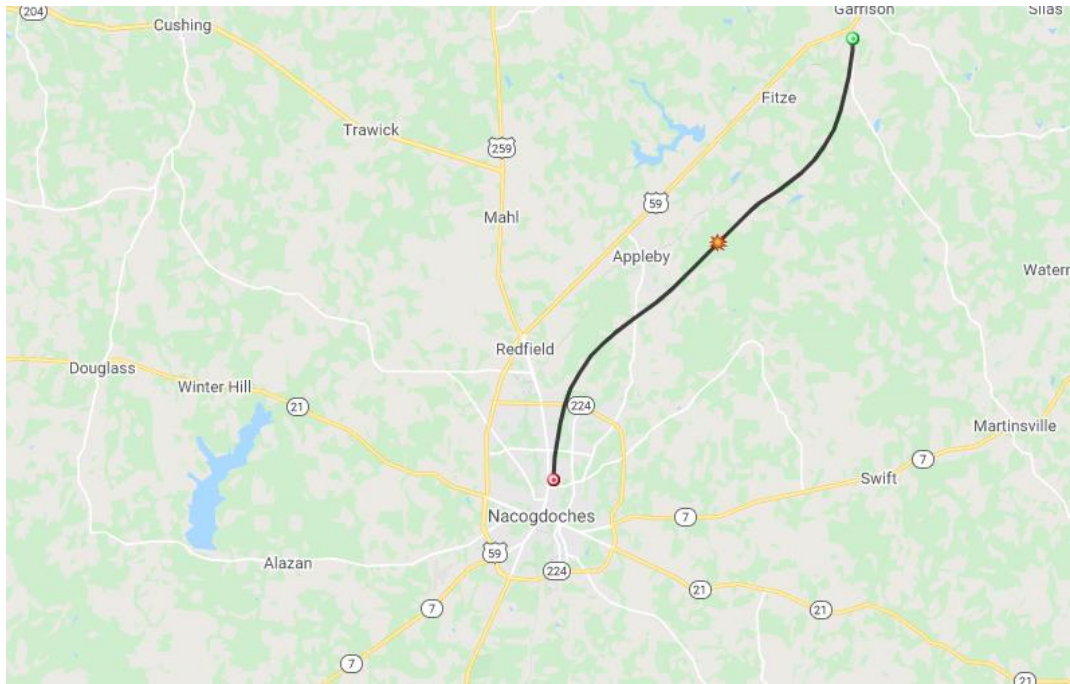
Figure 3.13: The predicted path if the burst altitude was 5000 m.
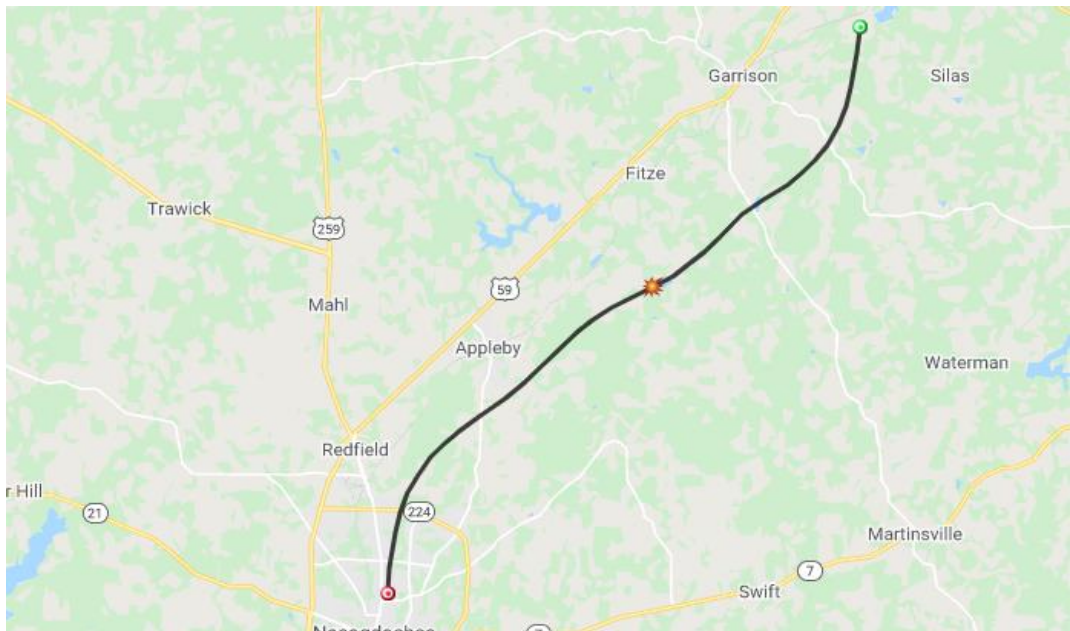
Figure 3.14: The predicted path if the burst altitude was 6000 m.
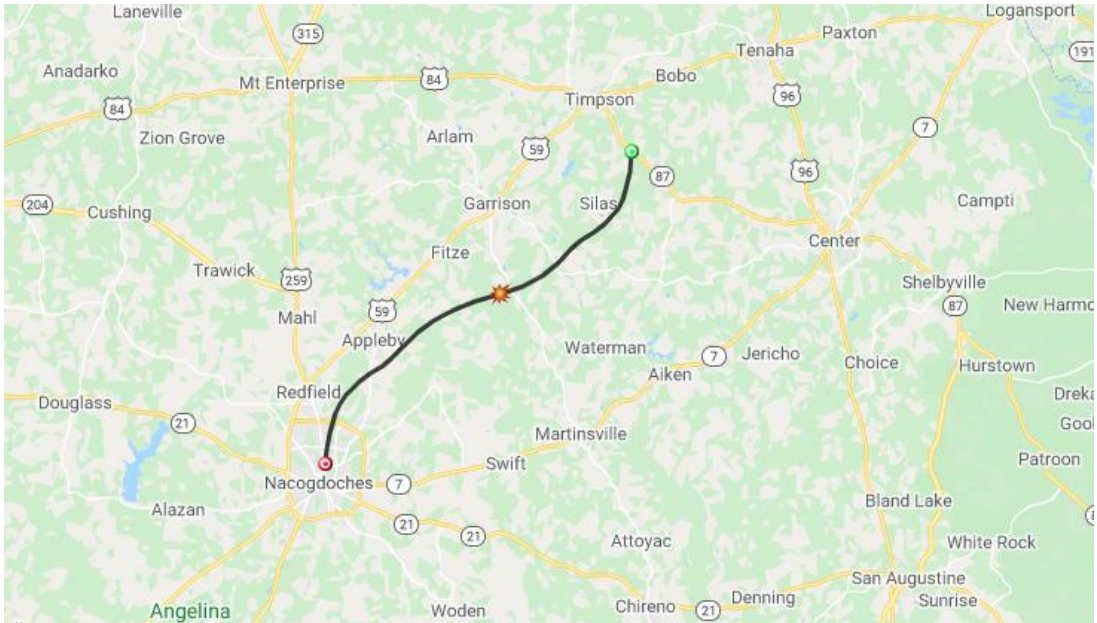
Figure 3.15: The predicted path if the burst altitude was 7000 m.
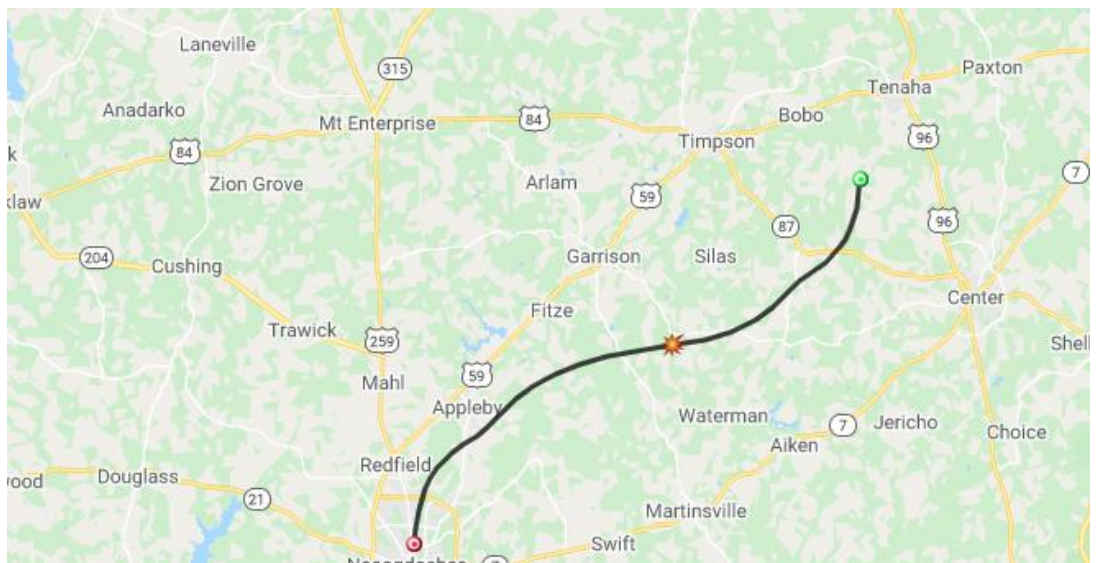
Figure 3.16: The predicted path if the burst altitude was 8000 m.
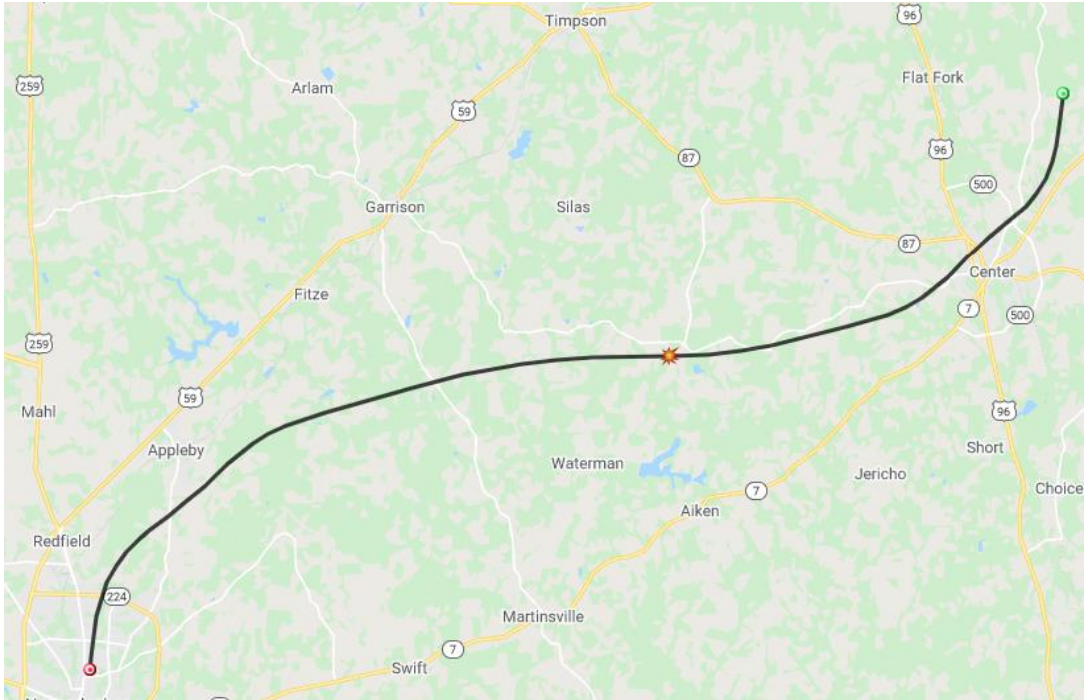
Figure 3.17: The predicted path if the burst altitude was 9000 m.
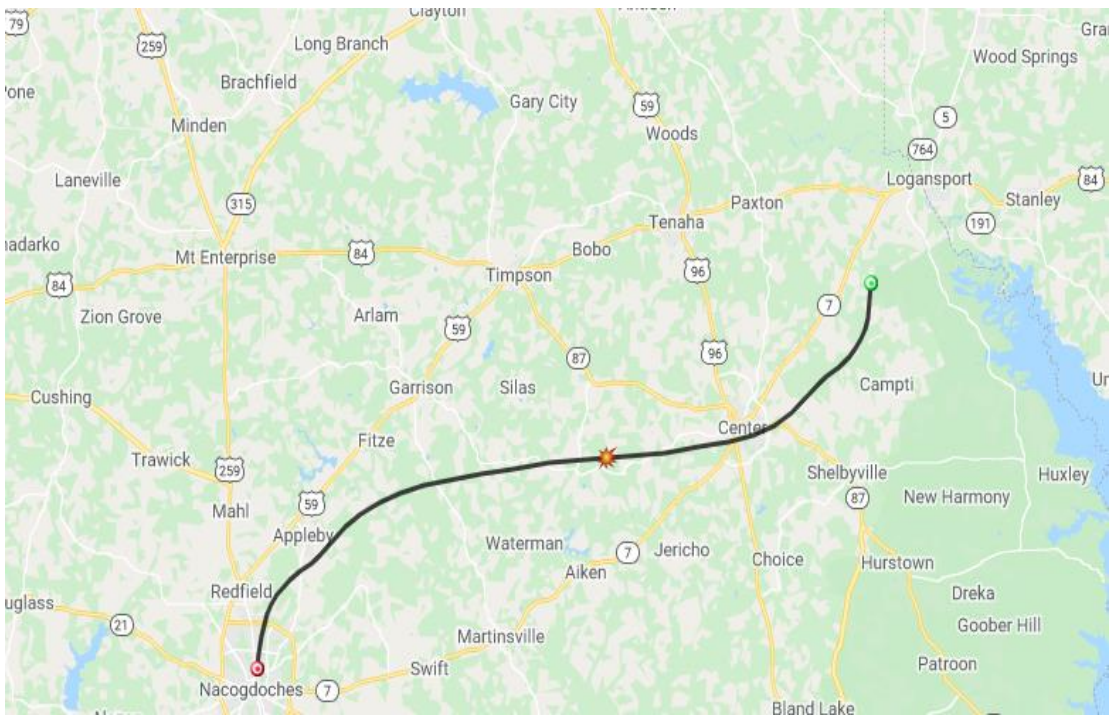
Figure 3.18: The predicted path if the burst altitude was 10,000 m.
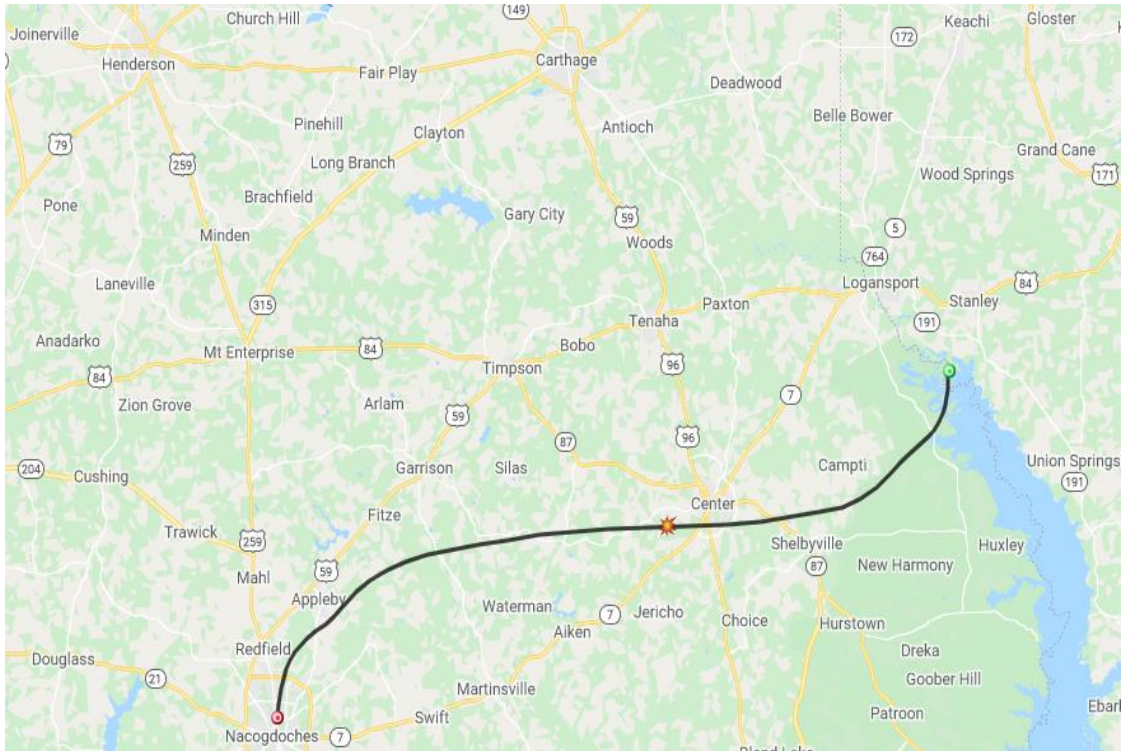
Figure 3.19: The predicted path if the burst altitude was 11,000 m.
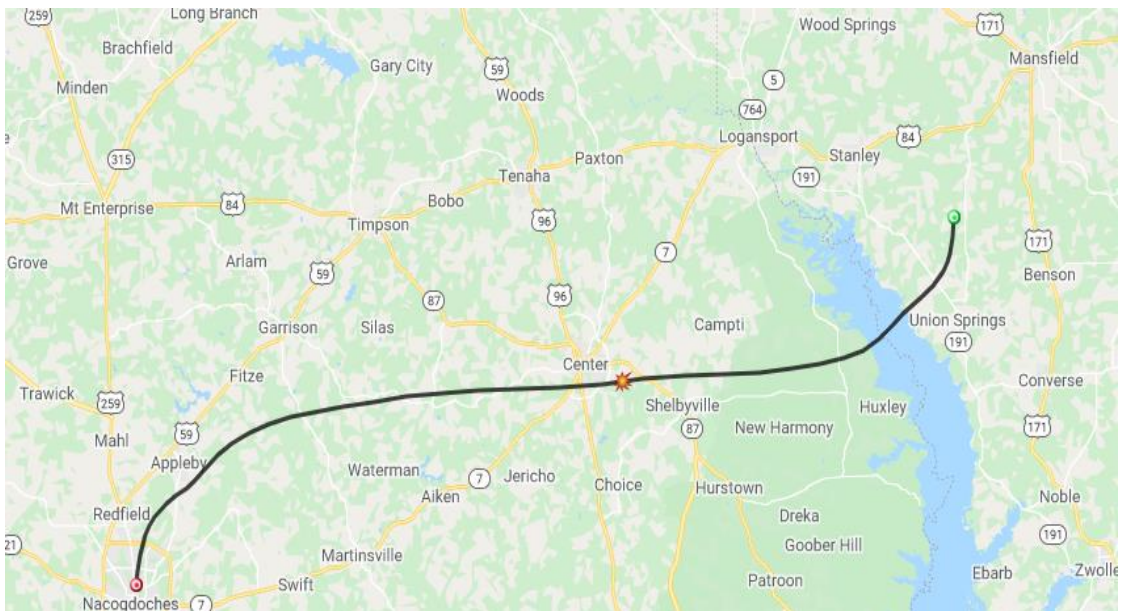
Figure 3.20: The predicted path if the burst altitude was 12,000 m.
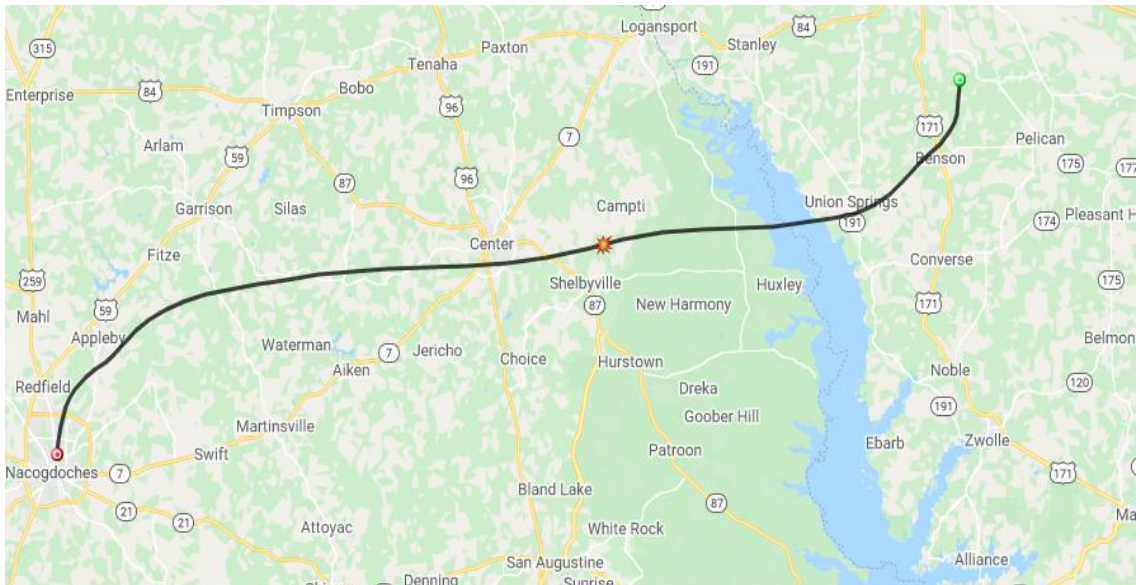
Figure 3.21: The predicted path if the burst altitude was 13,000 m.
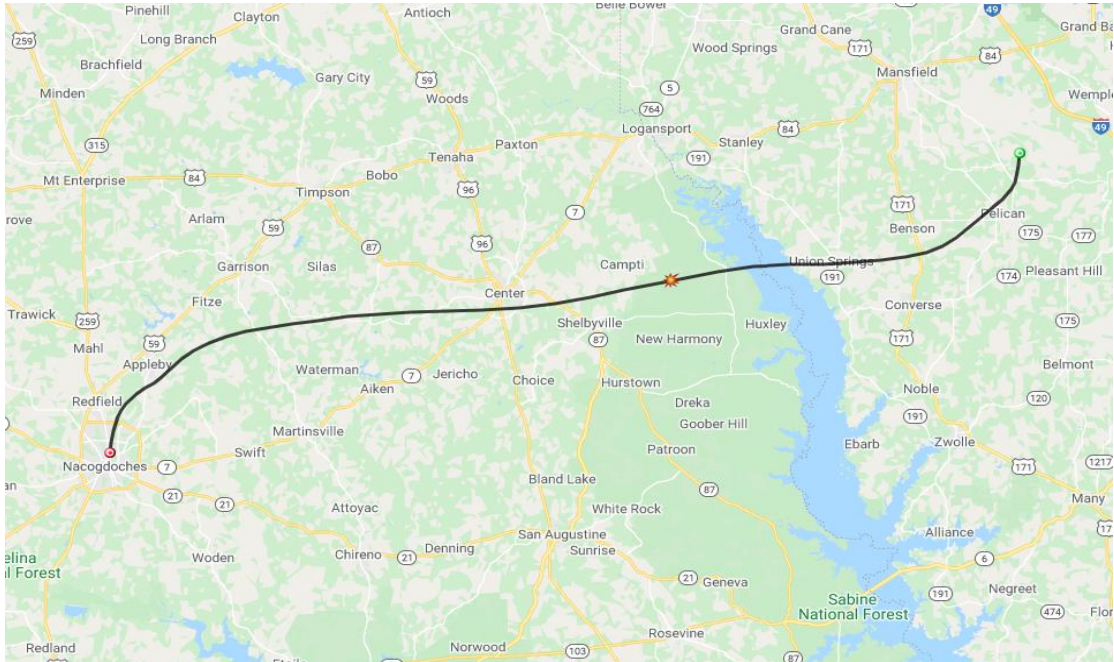
Figure 3.22: The predicted path if the burst altitude was 14,000 m.
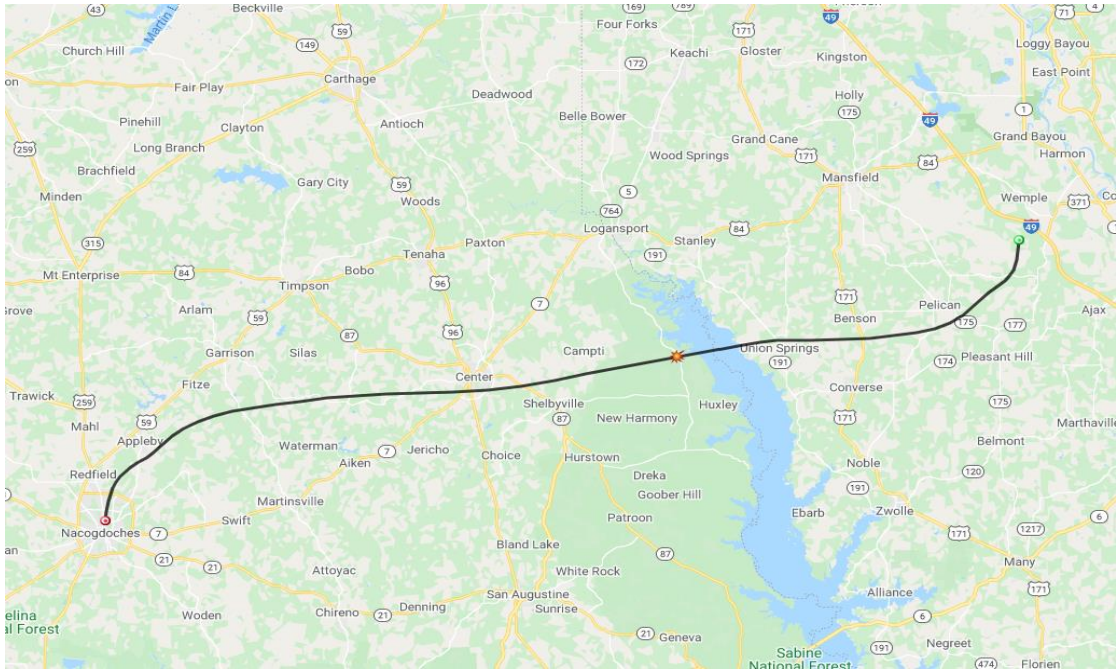
Figure 3.23: The predicted path if the burst altitude was 15,000 m.
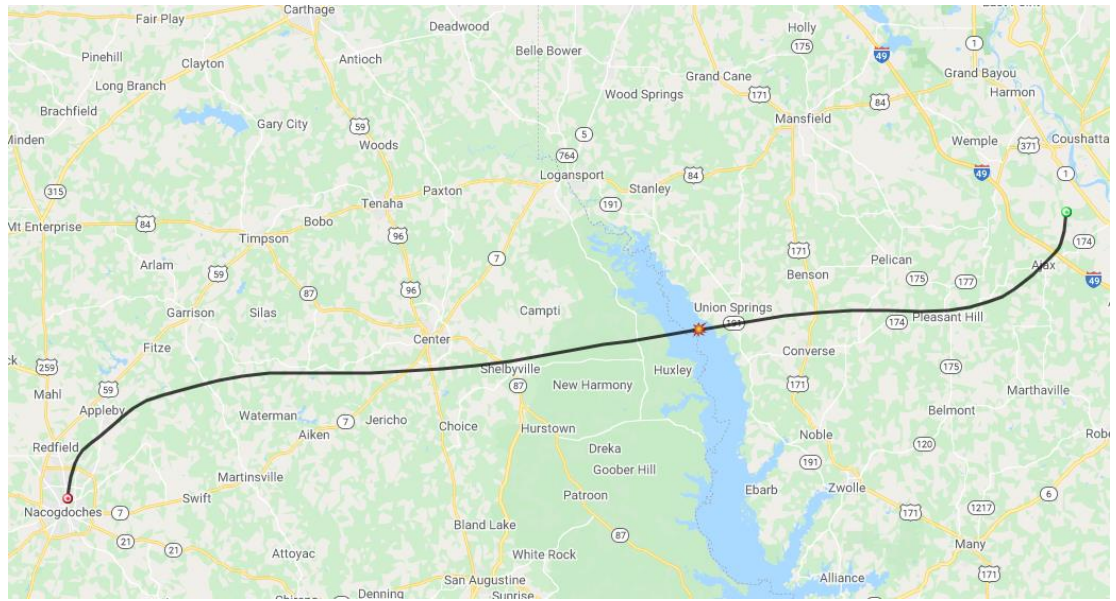
Figure 3.24: The predicted path if the burst altitude was 16,000 m.
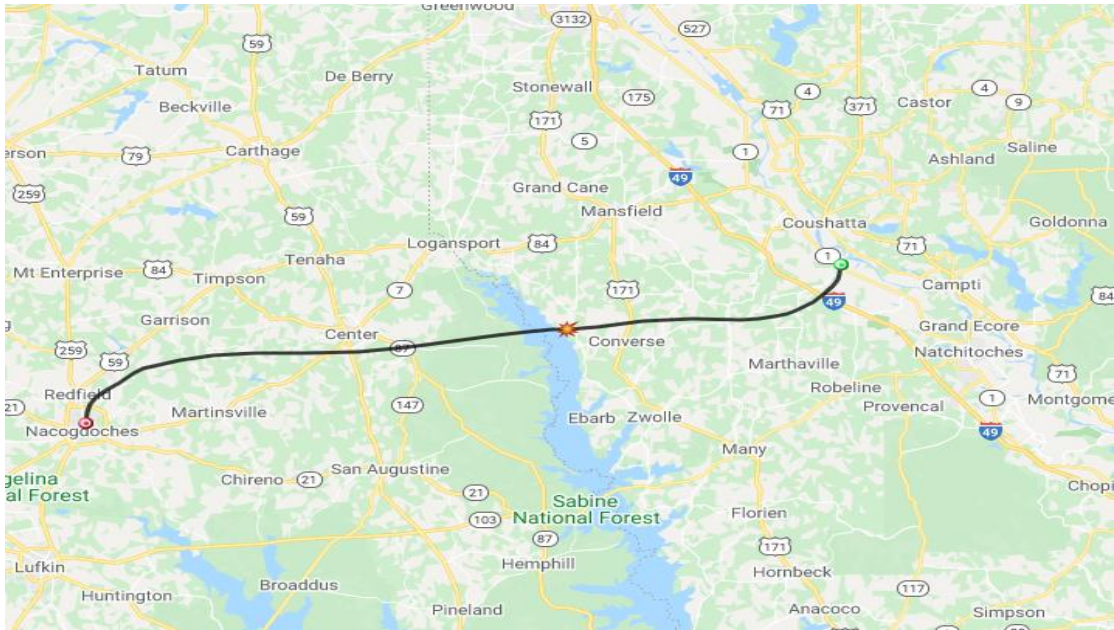
Figure 3.25: The predicted path if the burst altitude was 17,000 m.
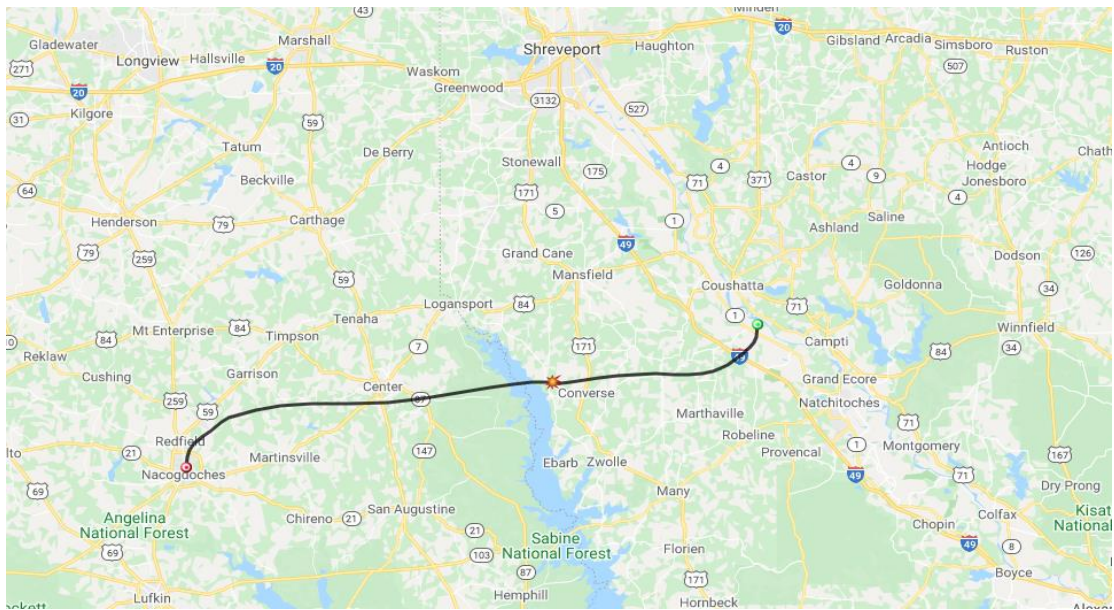
Figure 3.26: The predicted path if the burst altitude was 18,000 m.
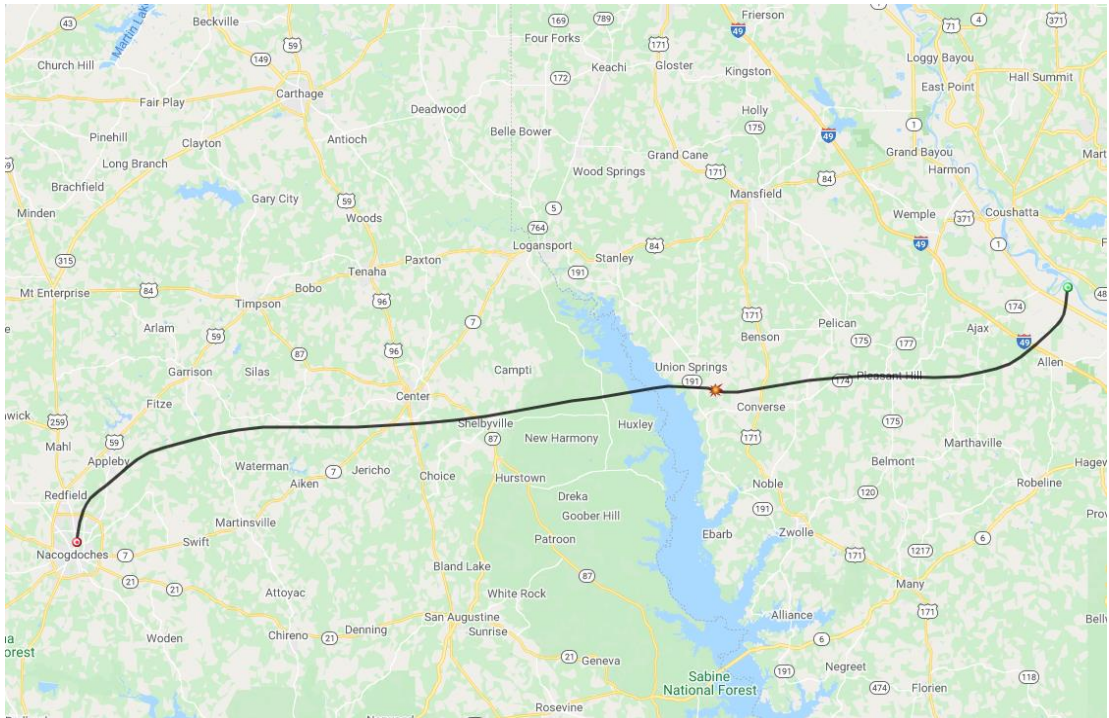
Figure 3.27: The predicted path if the burst altitude was 19,000 m.
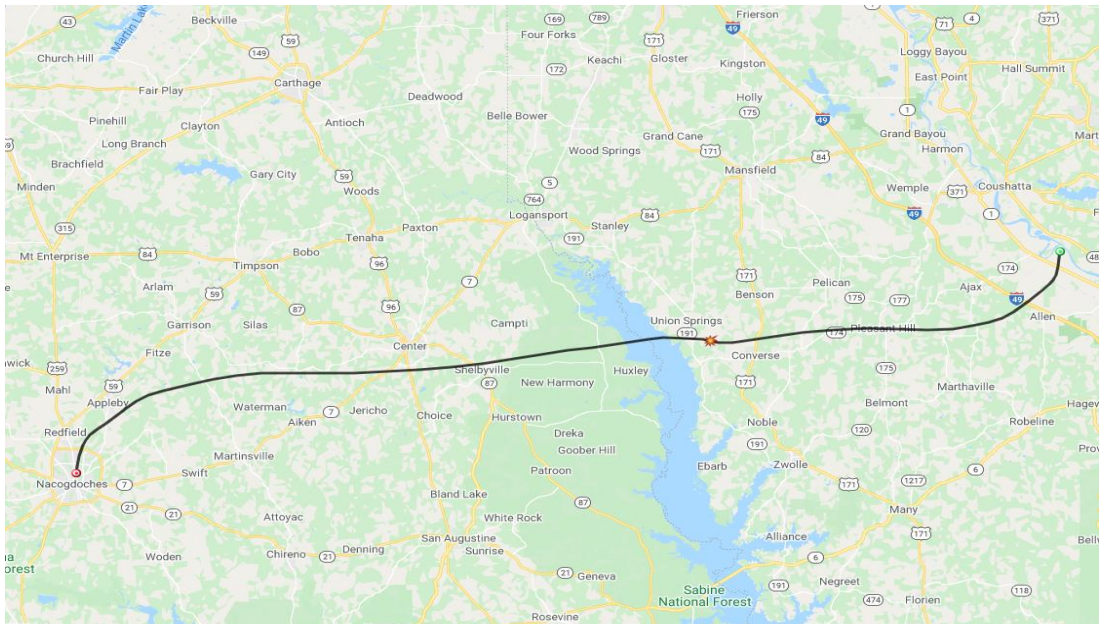
Figure 3.28: The predicted path if the burst altitude was 20,000 m.
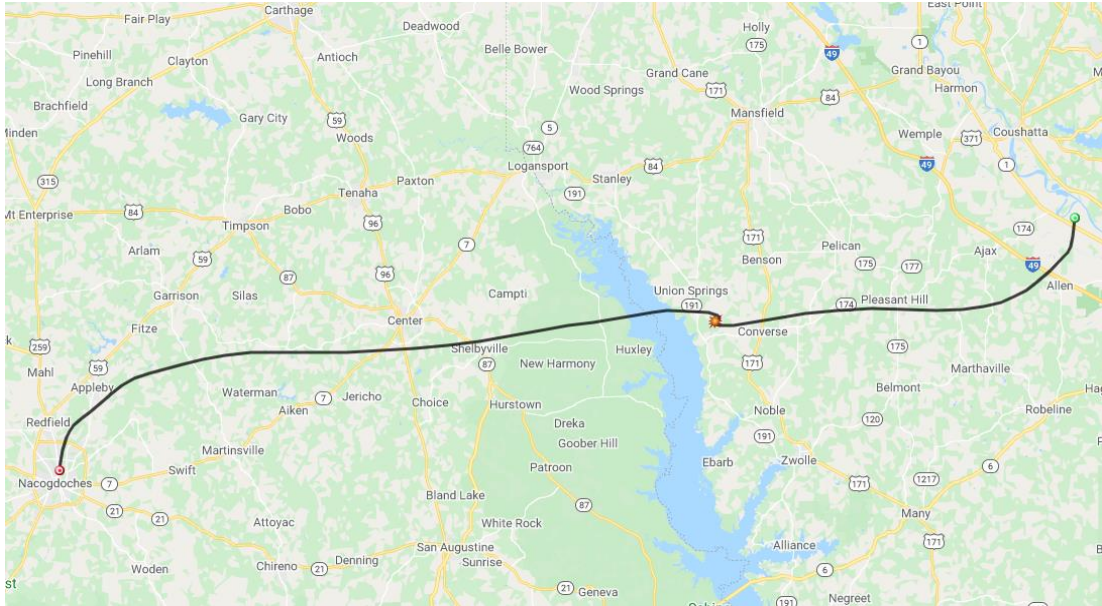
Figure 3.29: The predicted path if the burst altitude was 21,000 m.
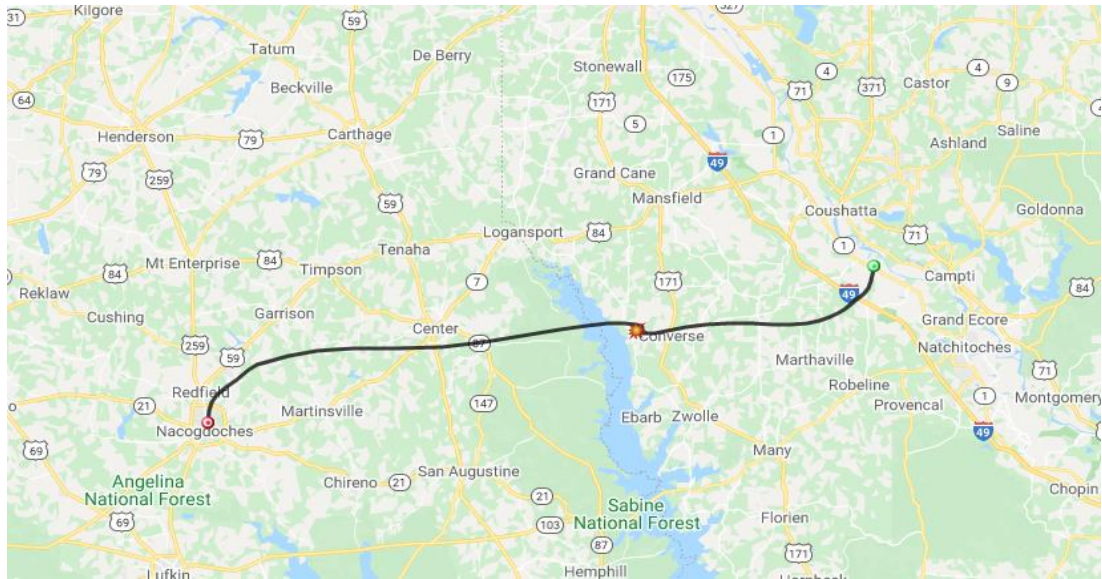
Figure 3.30: The predicted path if the burst altitude was 22,000 m.
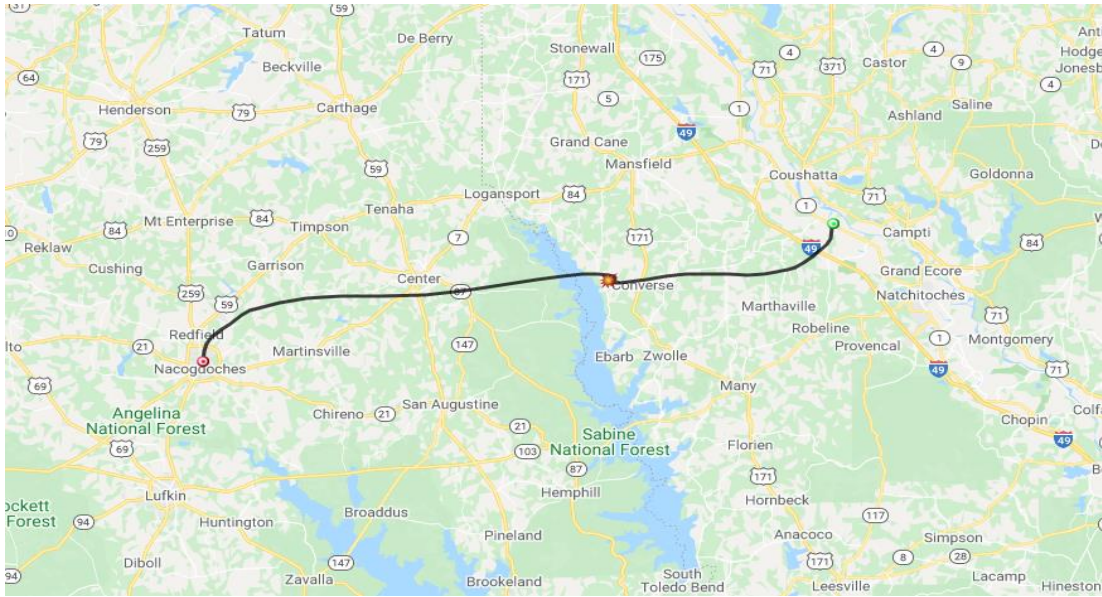
Figure 3.31: The predicted path if the burst altitude was 23,000 m.
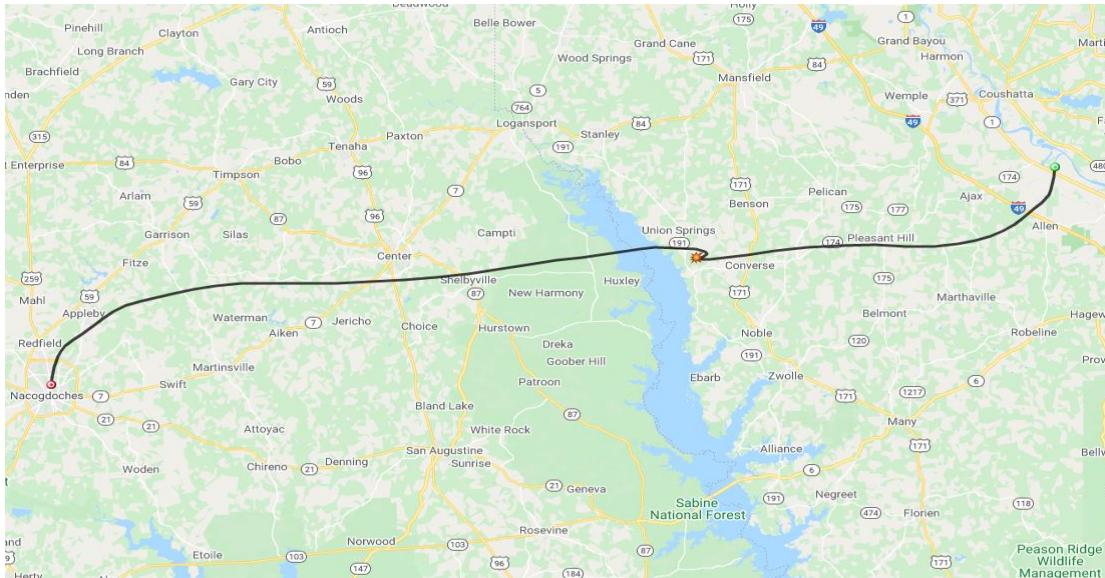
Figure 3.32: The predicted path if the burst altitude was 24,000 m.
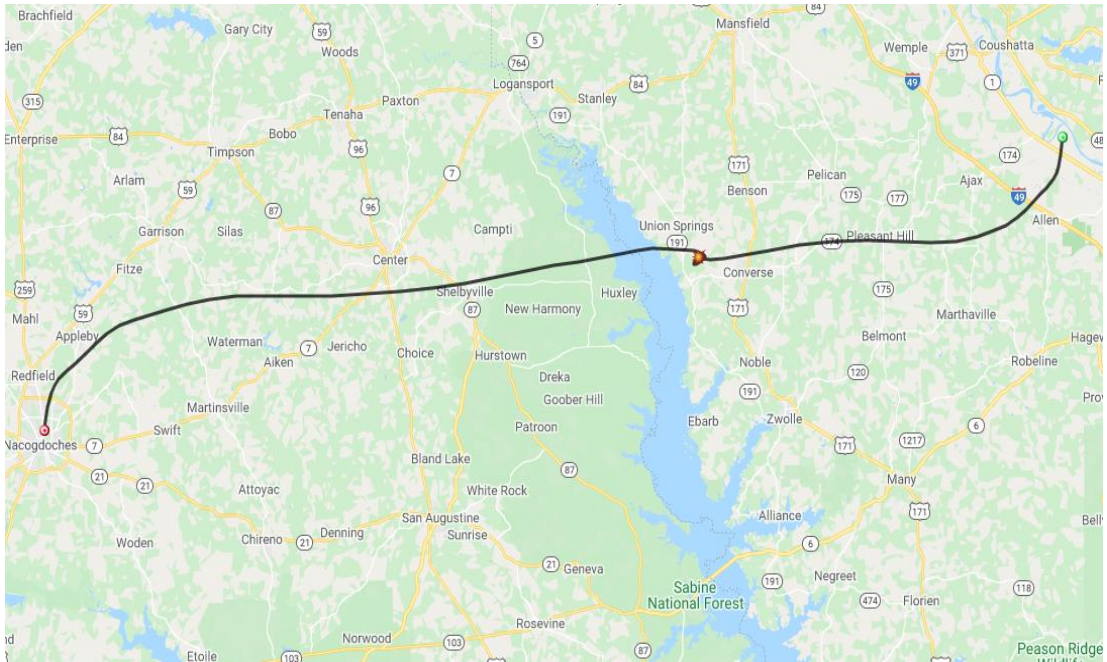
Figure 3.33: The predicted path if the burst altitude was 25,000 m.
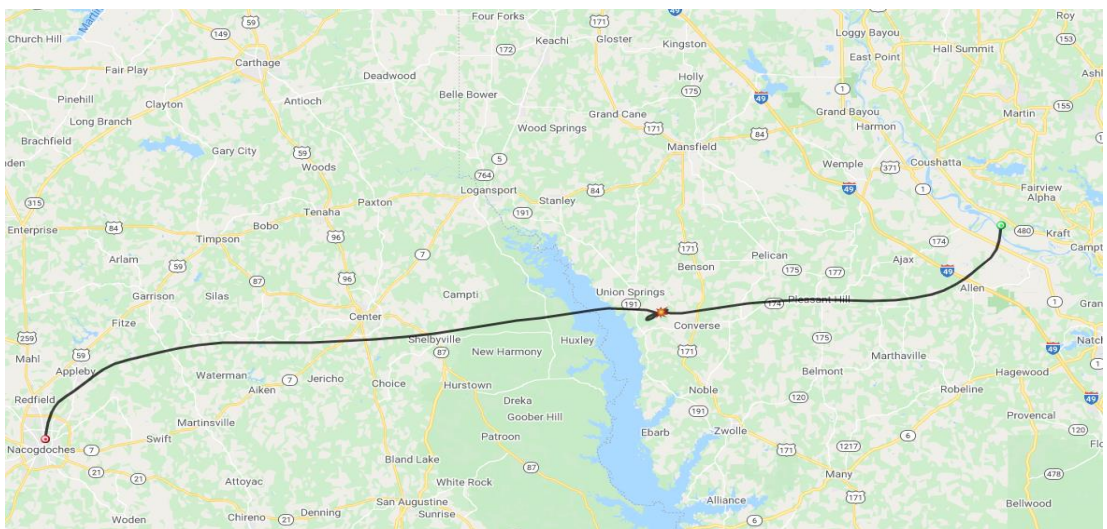
Figure 3.34: The predicted path if the burst altitude was 26,000 m.
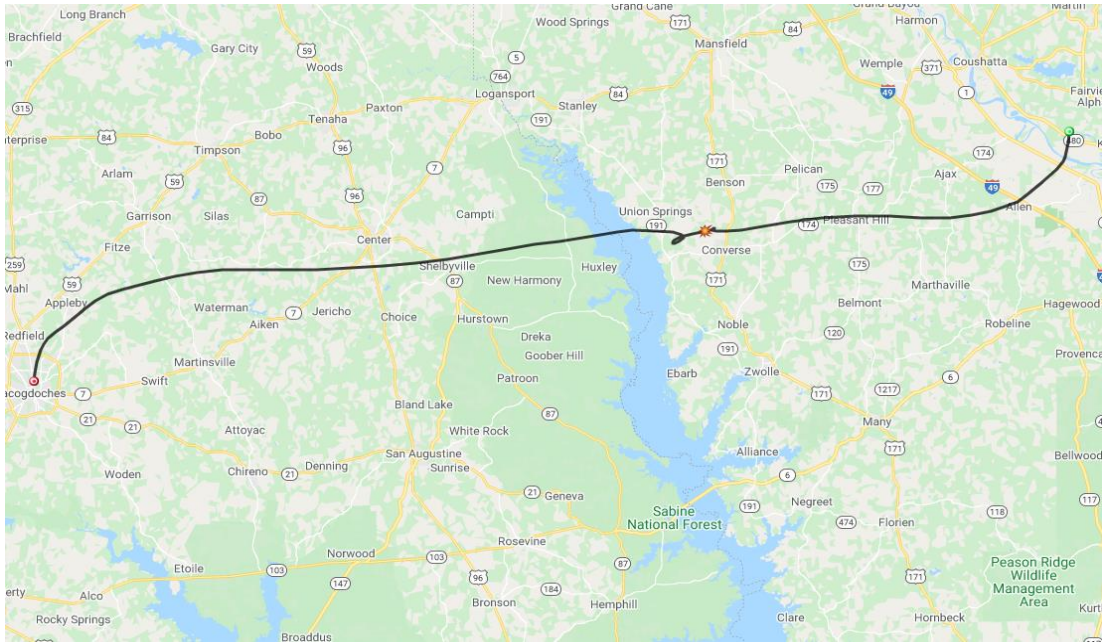
Figure 3.35: The predicted path if the burst altitude was 27,000 m.
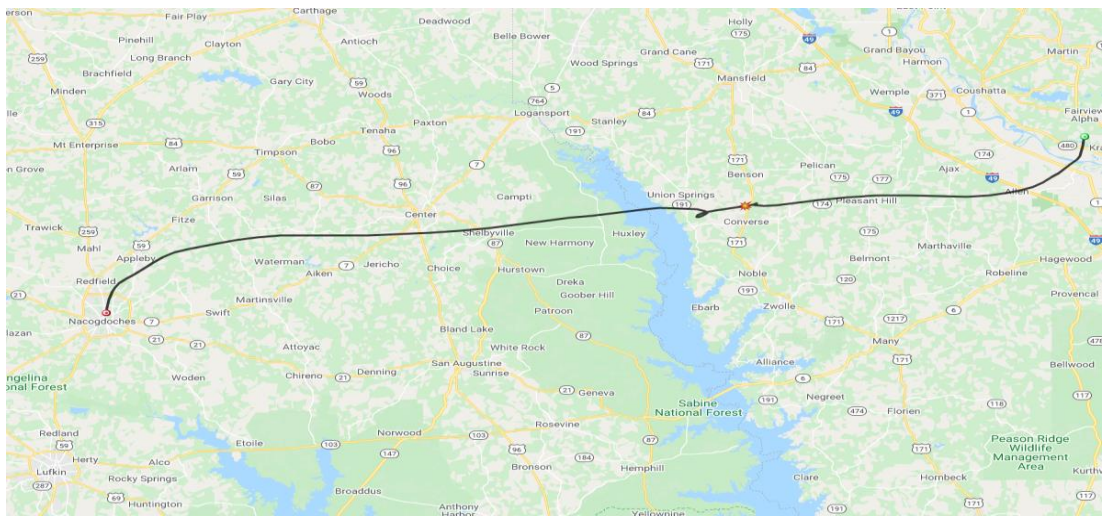
Figure 3.36: The predicted path if the burst altitude was 28,000 m.
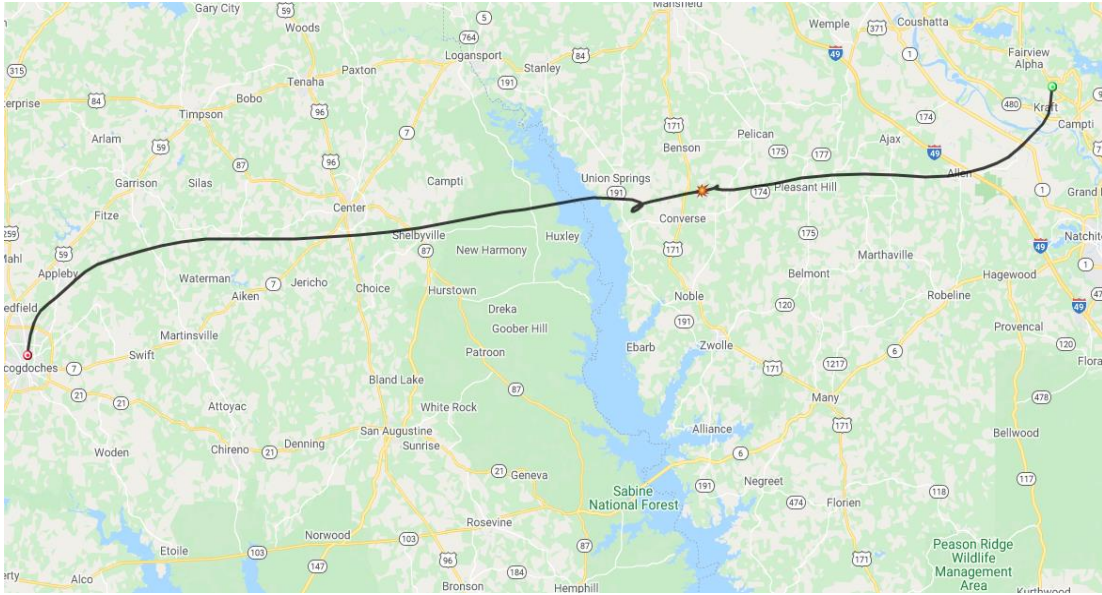
Figure 3.37: The predicted path if the burst altitude was 29,000 m.
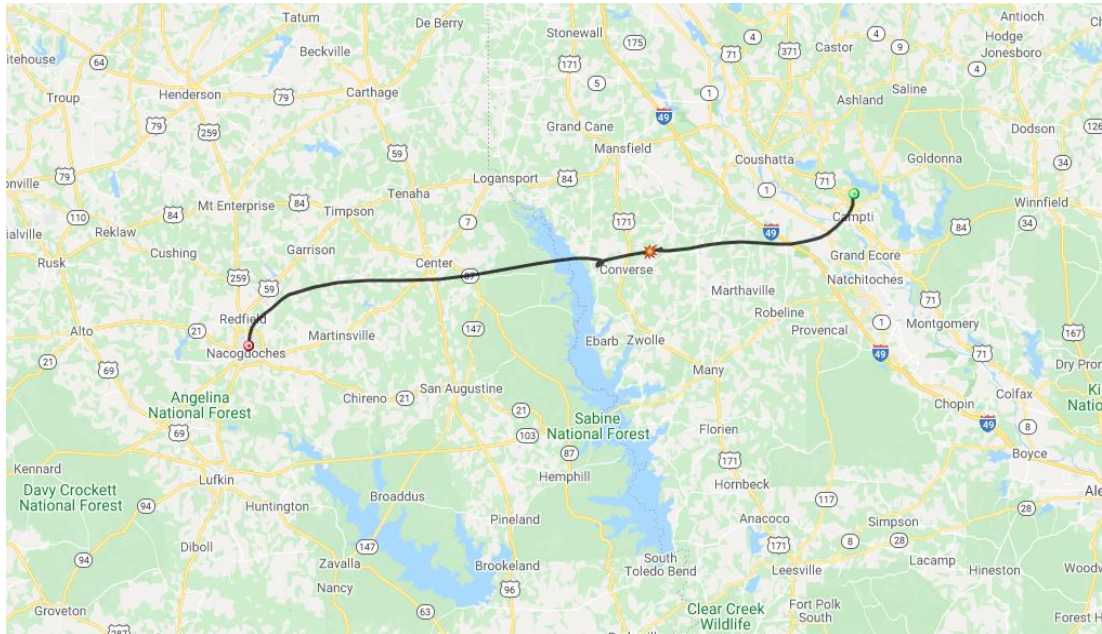
Figure 3.38: The predicted path if the burst altitude was 30,000 m.

Table 3.4: The data result from the prediction app.

Range (km)	Burst Altitude (meters)	Flight Time (hours)
16.7	3000	0.3167
20.5	4000	0.4167
25.7	5000	0.5167
31.9	6000	0.6167
38.2	7000	0.7000
45.5	8000	0.8000
55.7	9000	0.8833
64.3	10000	0.9833
75.4	11000	1.0667
87.1	12000	1.1500
98.6	13000	1.2333
108.7	14000	1.3167
116.4	15000	1.3833
126.9	16000	1.4667
131.1	17000	1.5500
133.9	18000	1.6167
135.3	19000	1.6833
135.5	20000	1.7667
134.7	21000	1.8333
134	22000	1.9000
133.8	23000	1.9667
134	24000	2.0333
135	25000	2.1000
136.9	26000	2.1667
139.5	27000	2.2333
142.5	28000	2.3000
145.8	29000	2.3500
144.6	30000	2.4167

Prediction Analysis

It was important to save images of all the predictions (Figures 3.9 through 3.36) because of the unique weather conditions that exist each day. From Table 3.4 we see that the range varies from 16.7 km to 144.6 km and the duration of the flight varies from 19 mins to 2hrs hours 25 mins for the range of burst altitudes considered. Figure 3.38 shows that range and the burst altitude are directly proportional, as burst altitude increases the range increases. Figure 3.39 shows that, as the burst altitude increases the time of flight increases for burst altitude from 3000 m to 30,000 m. They have an almost linear relationship.
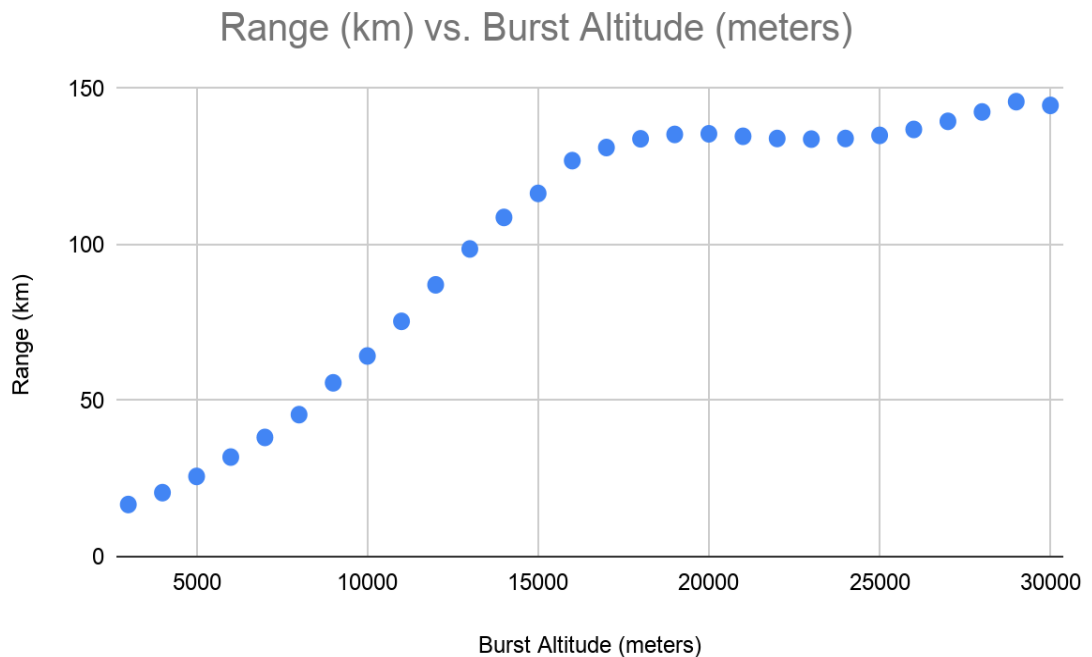
Figure 3.39: The plot of range versus burst altitude.
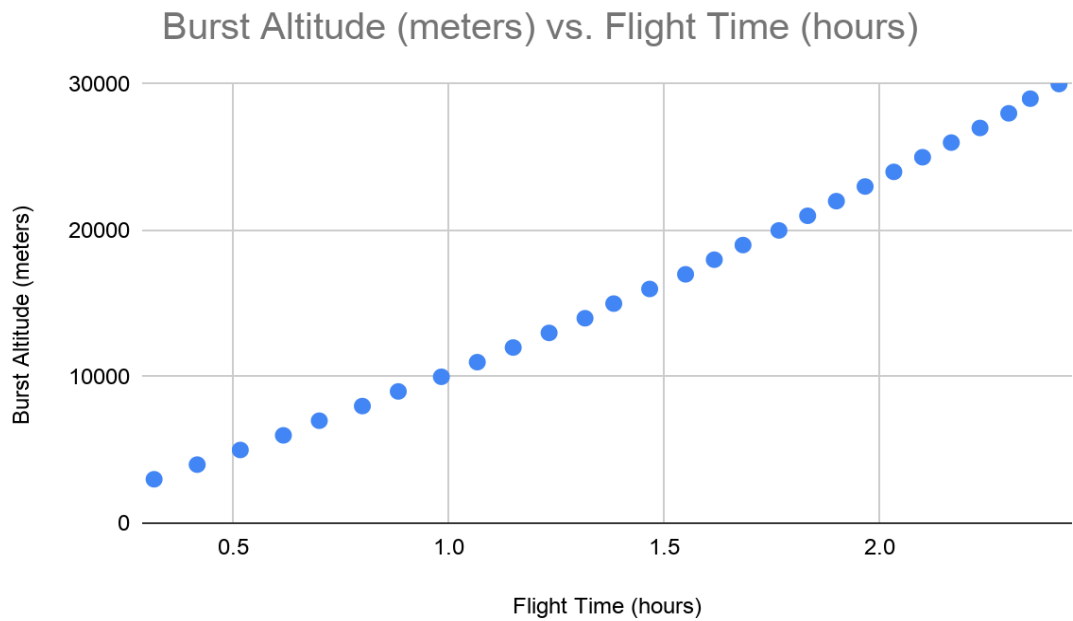
Figure 3.40: The plot of burst altitude(m) vs flight time(hours).

<u>Call to Federal Aviation Administration</u>

On the morning of March 11, 2021, we called the Federal Aviation Administration (FAA) at 1-877-487-6867 to request for a notice to airmen (NOTAM). We informed the responder that our location was OCH 4 nautical miles 060 degrees, LUK 27 nautical miles 003/007 with a launch location of 31.6194881°N and -94.6497343°W. We also provided the FAA with the weight of the payload and stated that we expected the maximum altitude of the experiment was going to be about 60,000 ft. We also described the estimated direction of travel of the weather balloon as generally east-northeast.

<u>Filling the Weather Balloon with Helium</u>

After the call to the FAA, we moved all equipment to be used for launch to the observation deck at the ED & Gwen Cole STEM Building on Thursday, March 11, 2021. A work station was set up, using two tables that were placed side by side and a drop cloth was laid on the table. Then the latex balloon was carefully laid on the table. With the help of Dr. Adams, Dr. Aul, Dr. Bruton and myself the Helium was then pumped via a hose gradually into the balloon. When the balloon attained the desired size, the balloon was tied firmly but carefully to prevent the helium from escaping. On the first attempt to tie the balloon, the balloon was ripped, meaning we had to tie the balloon with great care. Figure 3.40 and 3.41 show the preparation area and the process of carefully filling the latex balloon.

Figure 3.41: The filling of the balloon using Helium.

Figure 3.42: The balloon gradually gets filled with Helium.

After the balloon had been tied, the parachute was then attached to the balloon with the payload being attached to the connectors of the parachute below. It was an exciting moment, but alas the unimaginable occurred. Instead of ascending, the balloon descended from the observation deck to the ground. This was due to insufficient helium in the balloon. Figure 3.4 shows the moments before the first release attempt.

The helium in the balloon was released and refilled again. Much more helium was added to increase the diameter to about 1.6 meters, after which the balloon was tied and the parachute plus payload was tied up to the balloon. At exactly 11:23:29 AM, on March, 11 2021, I released my balloon and it ascended into the clouds. After several minutes it was out of sight. Figure 3.5 shows the moment prior to the second release attempt.

Figure 3.43: The first launch from the STEM building observation deck.

Figure 3.44: Refilling of the balloon after it descended from the observation

deck.

Actual Path of the Weather Balloon

From the downloaded data from the SPOT GPS, the balloon was released at 11:52:13 am at Burt Drive, Appleby Texas having a longitude and latitude 31.71° and -94.61° respectively. The balloon ascended with a speed of 29.62 mph horizontally and travelled for 5 hours 13 minutes in the atmosphere landing at 4:52 pm in a corn field at Jewel Hill Road, Waller Landing, Louisiana at a speed of 0.02 mph. The SPOT GPS could not transmit data for 2 hours and 17 minutes because at this point the altitude was beyond the altitude at which GPS devices are allowed to operate. This is referred to as the "COCOM limit". Comparing the actual path of the balloon with the predicted path, there is a strong correlation with the prediction path that had a burst altitude of 30,000 meters.

Table 3.5: The extracted data from SPOT GPS.

Time	Speed (MPH)	Latitude	Longitude
4:52:00 PM	0.02	32.0536	-91.60956
4:42:09 PM	8.1	32.05364	-91.60953
4:22:26 PM	24.49	32.01527	-91.61475
4:11:59 PM	66.04	31.97023	-91.66458
4:02:00 PM	73.46	31.98388	-91.85098
3:55:45 PM	30.7	32.02129	-91.97369
1:12:09 PM	98.04	31.97363	-93.3981
1:02:09 PM	84.13	31.95701	-93.6756
12:52:10 PM	77.07	31.94507	-93.91348
12:42:07 PM	66.54	31.93092	-94.13257
12:32:08 PM	54.46	31.9157	-94.32013
12:22:08 PM	40.39	31.89062	-94.47174
12:12:30 PM	32.38	31.83905	-94.56399
12:02:12 PM	23.94	31.77275	-94.6178
11:52:13 AM	29.62	31.71498	-94.61508
11:42:13 AM	13.7	31.64742	-94.64301
11:33:29 AM	0.06	31.6188	-94.64803
11:23:29 AM	0	31.6188	-94.64838

Data from the findmespot Gps Device

In **GPS** technology, the term "COCOM Limits" also refers to a **limit** placed on **GPS** tracking devices that disables tracking when the device calculates that it is moving faster than 1,000 knots (1,900 km/h; 1,200 mph) at an **altitude** higher than **18,000 m** (59,000 ft=11.2 miles).
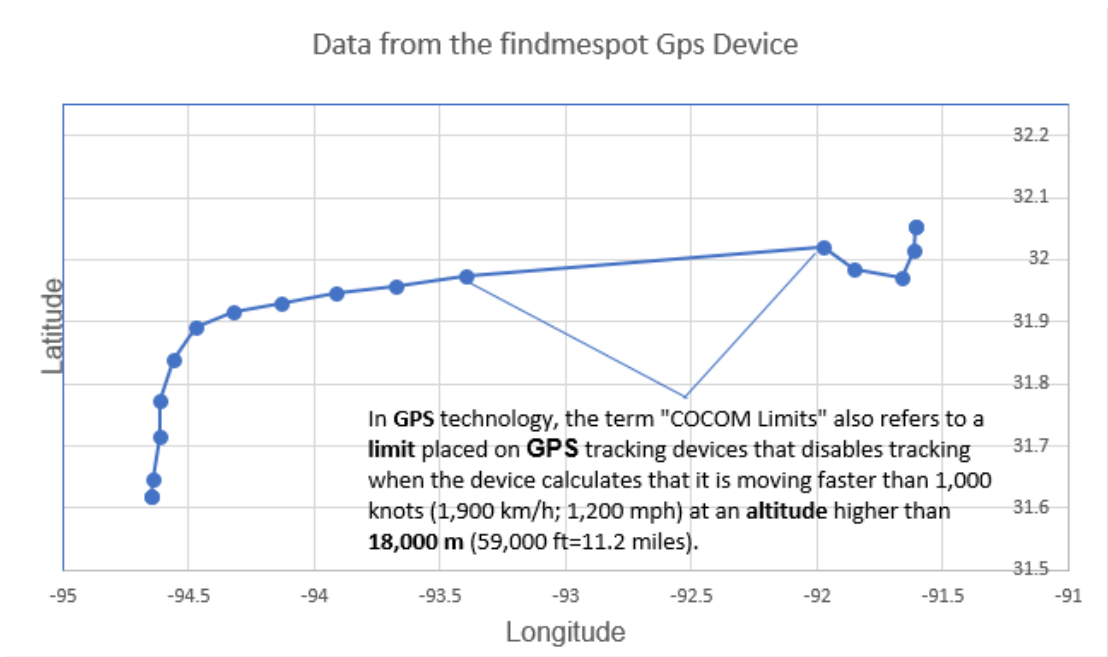
Figure 3.45: The plot of longitude versus latitude.
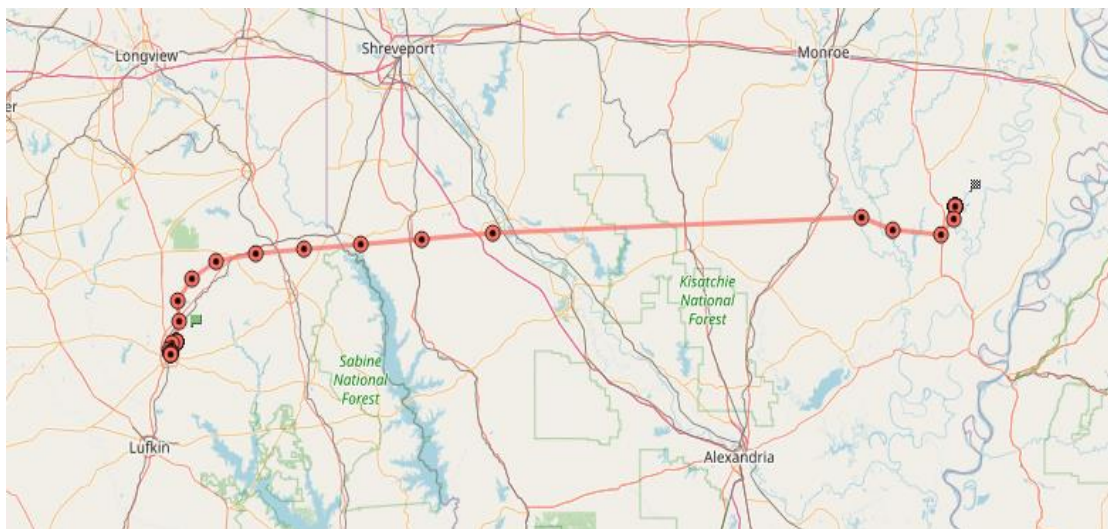
Figure 3.46: The actual path of the weather balloon as reported by SPOT GPS.

Figure 3.47: This is the figure that best matches the observation.

Figure 3.48: The plot of speed versus time.

.

The Geiger counter readings transmitted via the radiosonde lasted for seven minutes and the location was estimated to be around County Road 136, Pleasant Hill, Texas. The average while in flight via the radiosonde, the data radiation level is 0.0856 µSv/h. Table 3.6 and Figure 3.50 shows the Geiger radiation data and the plot of radiation versus time. We are hopeful that the payload will be recovered prior to the publication of this thesis so that more data can be reported.
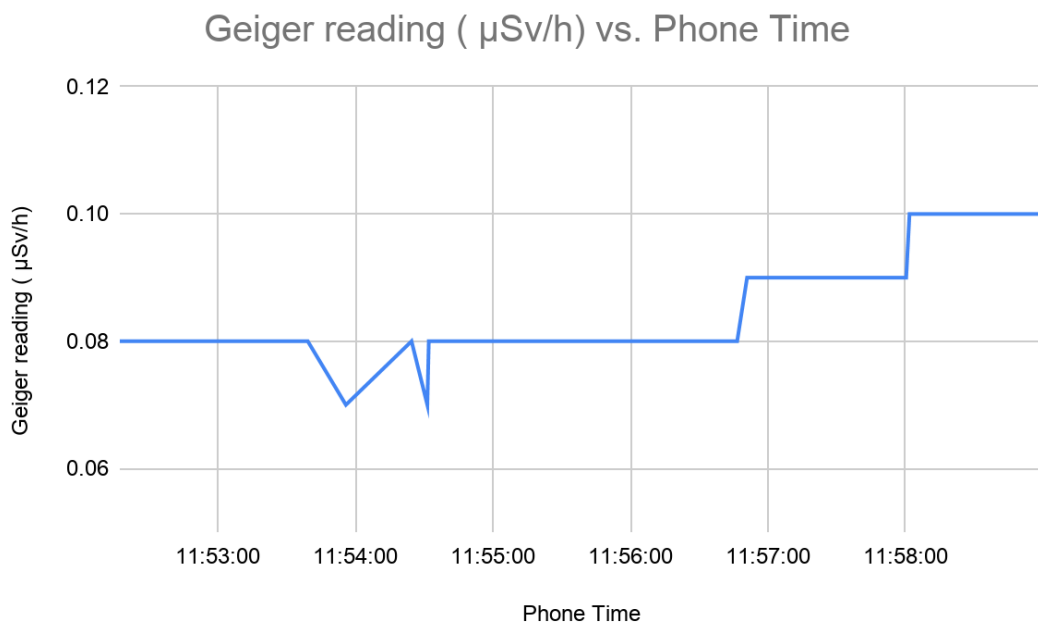
Figure 3.49: The plot of Radiation versus time.

Table 3.6: The Geiger radiation data.

Phone Time	Geiger reading (µSv/h)	Error
11:52:17	0.08	0.01
11:52:38	0.08	0.01
11:52:49	0.08	0.01
11:53:14	0.08	0.01
11:53:39	0.08	0.01
11:53:56	0.07	0.01
11:54:24	0.08	0.01
11:54:31	0.07	0.01
11:54:32	0.08	0.01
11:54:44	0.08	0.01
11:54:48	0.08	0.01
11:54:53	0.08	0.01
11:55:11	0.08	0.01
11:56:15	0.08	0.01
11:56:21	0.08	0.01
11:56:34	0.08	0.01
11:56:37	0.08	0.01
11:56:47	0.08	0.01
11:56:51	0.09	0.01
11:56:54	0.09	0.01
11:57:03	0.09	0.01
11:57:22	0.09	0.01
11:57:22	0.09	0.01
11:57:30	0.09	0.01
11:57:48	0.09	0.01
11:58:00	0.09	0.01
11:58:02	0.1	0.01
11:58:14	0.1	0.01
11:58:24	0.1	0.01
11:58:30	0.1	0.01
11:58:42	0.1	0.01
11:59:02	0.1	0.01

Table 3.7: Predicted altitude versus time.

Attitude (m)	t (sec)
0	0
100	50
200	100
300	150
400	200
500	250
600	300
700	350
800	400
900	450
1000	500
1100	550
1200	600
1300	650
1400	700
1500	750
1600	800
1700	850
1800	900
1900	950
2000	1000
2100	1050
2200	1100
2300	1150
2400	1200
2500	1250
2600	1300
2700	1350
2800	1400
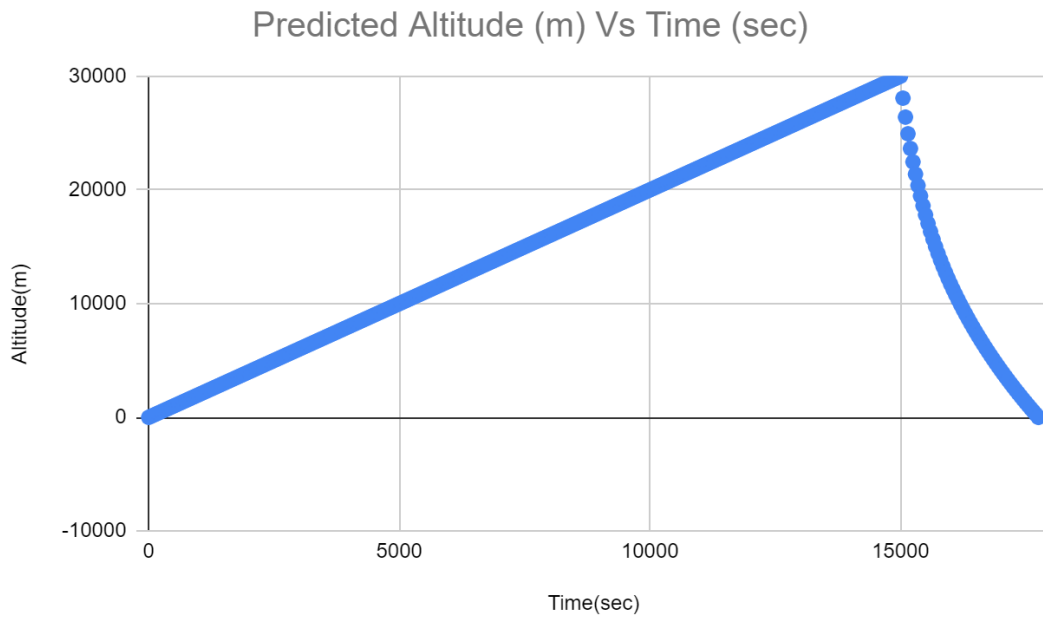
Figure 3.50: The predicted Altitude(m) Vs Time(sec).

Estimate Ascend Rate

The moment the weather balloon is launched, it begins to ascend into the stratosphere. We can estimate the ascend rate. Table 3.7 and figure 3.51 shows the data of altitude, time and their plot respectively. After the balloon had landed, we changed the ascend rate for the prediction module to match the result from the SPOT GPS device. Based on these new predictions the estimated ascend rate is as follows.

$$V_{Ascend\ rate} = \frac{30000}{time\ going\ up} \dotfill (12)$$

$$V_{Ascend\ rate} = \frac{30000}{15000}$$

$$V_{Ascend\ rate} = 2.0\ m/s.$$

CHAPTER FOUR

RESULTS AND CONCLUSION

Summary of Result

     The research was successful in that we were able to use a long-range radio transmitter to obtain valuable data such as radiation counts per minutes, speed, longitude, latitude, and speed about the HAB while in flight and landing. We were able to demonstrate that an instrument that cost less than $1000 can help collect Geiger counter readings up to 20 miles high. We were able to build the payloads that can be recycled with low cost and low risk which is difficult to achieve by satellites. We were able to analyze the data collected which are presented in Chapter Three.

Juxtaposing Results Obtained with Other Research carried out in this Field

     The research group of the Balloon Group at the Institute of Space and Astronautical Science (ISAS) have been engaged in the development of a light balloon to go to higher altitudes since 1991. On May 23, 2002, they launched a 60,000 m^3 balloon and the balloon reached an altitude of 53.0 km. This is the highest altitude ever reached by a balloon. By contrast, our experiment reached an altitude of about 30.0 km.
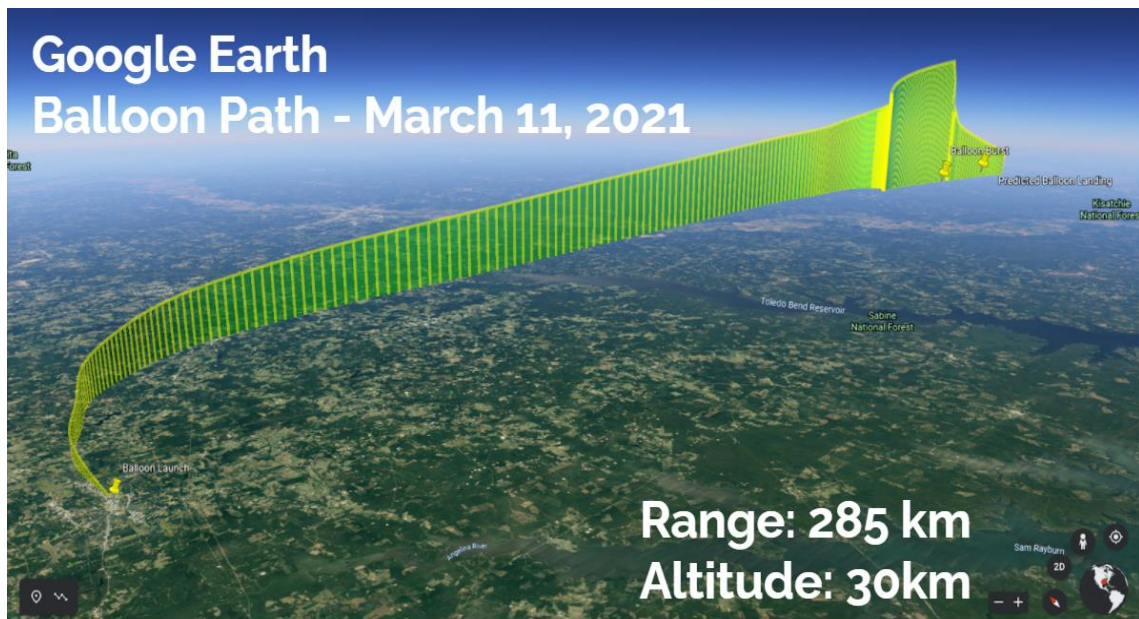
Figure 4.1: Google Earth of our flight path.

Based on the data collected by the Integrated Global Radiosonde Archive, the fastest jet stream ever recorded on Earth by a weather balloon is 115.7 m/s (416.5 km/h; 258.8 mph) and the altitude recorded was 10.4 km. The reading was taken near Yonago in Tottori, Japan, from where the balloon launched on February 5th, 2004. By contrast, from the data extracted from SPOT GPS, our weather balloon speed started from 0 mph (mile per hour) to a maximum speed of 98.04 mph. The balloon travelled at a progressive speed rate, and the weather condition was favored.

The payload for this research traveled farther than any of the 6 previous Near Space projects conducted at Stephen F. Austin State University in the Department of Physics, Engineering, and Astronomy. The total distance travelled was 285 km for this research. We were able to recover seven minutes

80

of radiation data starting from the time of launch until the payload reached County Road 136, Pleasant Hill, Texas, after which no data was transmitted. The average radiation level is 0.0856 µSv/h.

The ascend rate used for the prediction modelling was initially 5.0 m/s but after the balloon was launched we noticed it was not rising at the initial predicted rate. In order for the prediction rate to better match the actual rate we adjusted the prediction model to match the results from the SPOT GPS device. Based on these new predictions our ascend rate was estimated to be 2.0 m/s.

In conclusion, development of a balloon flying at high altitude is one of the most attractive trials for balloon technology. At Stephen F. Austin State University, Department of Physics, Engineering, and Astronomy has launched a total of six near space projects between 2015 and 2020. Many of the objectives were met as stated in chapter one such as using long-range radio transmitters to collect some radiation data, predicting the path of the high-altitude balloon, building payloads that can be recycled with low cost and low risk, testing and analyzing the results obtained from the device and make future predictions about the nature of radiation in the Earth's atmosphere, demonstrating that an instrument that costs less than $1000 can help collect Geiger counter readings up to 20 miles high, obtain the location (latitude and longitude), altitude, and speed.

BIBLIOGRAPHY

1.   "High-Altitude Balloon Experiments at the Indian Institute of Astrophysics." Margarita, S., Akshata, N., Sreejith, A., Joice, M., Mayuresh, S., Ambily, S., Nirmal, K., Talnikar, S., Shripathy, H., Prakash, A., and Jayant M., (2014).

2.   "A High-Altitude Balloon Platform for Space Life Sciences Education." Jordan, M., Tristan, C., Alex, H., Elizabeth, T., Sonali, V., Kaixin, Cui., Boguraev, A., Molly, H., Aimee, J., Emily, J., Andrew, J., Brooke, S., Jamie, S, Nhung, T., and Jon, R., doi.org/10.2478/gsr-2019-0007 | Published online: 27 Nov 2019.

3.   "Rays and Particles University of Virginia Lecture Notes" University of Virginia Physics Department (2014).

4.   "The Montgolfier Brothers, and the Invention of Aviation." Gillispie, C. (1983) (Princeton University Press, USA), p. 45, 46, 178, 179, 183- 185.

5.   "An overview. Advances in Space Research", Smith I.S. (2002)

6.   "The longitude and latitude of Stephen F Austin University." tools.wmflabs.org/geohack/geohack.php?pagename=Stephen_F._Austin_State_ University&params=31.62139_N_94.64917_W_

7.   "High-Altitude Balloon-Based Sensor System Design and Implementation." (2020) Zhanchao, W., Min, H., Lulu, Q., Baowei, Z., and Guangming, W.,.

8.   "The magnetic and electric deviation of the easily absorbed rays from radium", E. Rutherford (1906).

9.   "Radio-Transmission of Cosmic Ray Data from the Stratosphere" (1935). "Vernoff, S.

10.   "The engineering toolbox", Jan. 15th, 2021 engineeringtoolbox.com/standards-atmosphere-d_604.ttml

11.   "Development of the highest altitude balloon"(2002) T.Yamagamia, Y.Saito, Y.Matsuzaka, M.Namiki, M.Toriumi, R.Yokota, H.Hirosawa, K.Matsushima.

12.   "Cost-effective platforms for Near-space research and experiments",(2017) By K.Gozlan, Y.Reuveni, K.Cohen, B.Ben-Moshe, E.Berliner.

13.   "Overview of the Integrated Global Radiosonde Archive" Imke Durre, Russell S. Vose , and David B. Wuertz 1 (2006).

14.   "CUSF Landing Predictor 2.5", UK High Altitude Society, Apr. 2021, predict.habhub.org.

15.   "Pocket Geiger Radiation Sensor - Type 5 - SEN-14209", SparkFun Electronics, Apr. 2021, sparkfun.com/products/14209.

16.   "High-Altitude Balloon Experiments at the Indian Institute of Astrophysics." Margarita, S., Akshata, N., Sreejith, A., Joice, M., Mayuresh, S., Ambily, S., Nirmal, K., Talnikar, S., Shripathy, H., Prakash, A., and Jayant M., (2014).

17.   "Geiger–Müller tube", Wikimedia Foundation, Nov. 2019, en.wikipedia.org/wiki/Geiger%E2%80%93M%C3%BCller_tube.

18.   "Sparkfun start something", Sparkfun, Feb. 2021, sparkfun.com/products/14209.

19. "Arduino IDE 1.8.13", Arduino Team, Apr. 2021, arduino.cc/en/software.

20. "Serial Bluetooth Terminal -Apps on Google Play", March 9th, 2021, play.google.com/store/apps/details?id=de.kai_morich.serial_bluetooth_terminal& hl=en_US&gl=US.

21. "Automate", google play, March 30th, 2021 play.google.com/store/apps/details?id=com.llamalab.automate&hl=en_US&gl=U S.

22. "Radioactivity: Weak Forces".(2020) *Radioactivity*. EDP Sciences. Retrieved 4 March.

23. "Gamma ray", Wikipedia, March 25th, 2021, en.wikipedia.org/wiki/Long_range_alpha a.

24. "Launching, tracking and flying high altitude weather balloons in the Rochester, NY area" March 16th, 2021. overlookhorizon.com/how-to-launch-weather-balloons/parachutes/.

25. "Mill-max", March 16th, 2021. mill-max.com/products/new/printed-circuit-board-pcb-pins

26. "Center for science for education" March 15th, 2021, scied.ucar.edu/learning-zone/atmosphere/weather-balloons.

VITA

After completing her Bachelor of Science degree in Engineering Physics from Obafemi Awolowo University Ile-Ife, Nigeria in 2015, Ayodeji Akinuliola embarked on a one-year post-graduation volunteering service. In 2017, She joined Transilient Technologies in Lagos, Nigeria where she worked as an Electrical Engineer. After two year of full-time employment with Transilient Technologies, Ayodeji decided to bolster her knowledge and contribute to Physics and Engineering by relocating to Nacogdoches, Texas, United States to pursue a Master of Science degree in Physics and Astronomy at Stephen F. Austin State University (SFA) which commenced Fall 2019. As a graduate student at SFA, Ayodeji was a graduate teaching assistant and served as a Senator for the graduate school under the auspices of the Student Government Association. In the Spring of 2021, she was conferred a Master of Science degree in Physics and Astronomy at SFA.

Permanent Address: 1707 Hallmark Avenue North

Oakdale Mn, 55128

Style MLA form

This Thesis was typed by Ayodeji O. Akinuliola